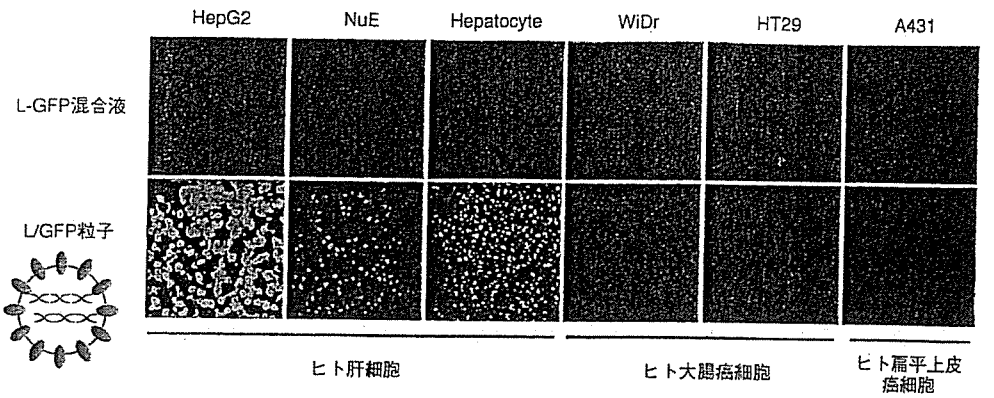

図3●培養細胞レベルでのGFP遺伝子のヒト肝細胞特異的導入

L粒子とGFP発現プラスミドを混合（L-GFP混合液），あるいはL粒子にGFP発現プラスミドをエレクトロポレーションで封入（L/GFP粒子）したものを各種培養細胞に血清存在下で添加した．L/GFP粒子を添加した場合は，ヒト肝がん由来細胞株（HepG2，NuE）およびヒト肝細胞株（Hepatocyte）ではGFPに由来する蛍光が観察されたが，ヒト大腸がん由来細胞株（WiDr，HT29）やヒト扁平上皮がん由来細胞株（A431）では蛍光が観察されなかった．一方，L-GFP混合液ではいずれの場合も蛍光は観察されなかった

残り10％がリン脂質である．

L粒子は，昆虫細胞を用いて，適当な分泌シグナルとプロモーターを組み合わせることで，粒子の形で効率よく細胞外に分泌生産することも可能である[10]．この場合も得られる粒子のサイズは90 nm程度である．どのような生産法が最適化は，利用方法により異なるため，選択することが可能である．

3. 中空バイオナノ粒子によるピンポイト遺伝子デリバリー

中空バイオナノ粒子を遺伝子のピンポイントデリバリーに用いるには，まず粒子内に遺伝子を封入する必要がある．現在のところ，封入は2つの方法で行われている．すなわち，エレクトロポレーションによる方法とリポソームを用いた方法である．エレクトロポレーションでは，高電圧パルスを付加することで，粒子膜の構造を瞬間的に乱して遺伝子を粒子内に取り込ませる[11)~13)]．リポソームを用いた方法では，まずリポソームに遺伝子を取り込ませた後，L粒子と融合させることで封入が可能である[14)]．リポソーム法では，微粒子を含む巨大な物資の封入も可能である．遺伝子封入L粒子による特異的な遺伝子導入について，まずモデル系としてクラゲの緑色蛍光タンパク質（GFP：遺伝子導入によりタンパク質が生産されると緑色蛍光が観察できるため，判定がしやすい）の遺伝子を用いて検討した．遺伝子封入L粒子を各種の培養細胞に血清存在下で添加して導入実験を行ったところ，図3に示すように，ヒト肝細胞培養株およびヒト肝がん由来細胞株（HepG2やNuE）でのみGFPの発現による緑色蛍光が観察された．このようにL粒子は，肝細胞特異的かつ高効率な遺伝子導入に有効であることが明らかとなった[11)~13)]．

そこで，次のステップとして，生体内でL粒子による遺伝子のピンポイントデリバリーが可能か，実験動物を用いて検討した．すなわち，1匹のヌードマウス背部皮下にヒト肝細胞がん由来の細胞株（NuE：標的）とヒト大腸がん由来細胞株（WiDr：対照）を1つずつ移植し，GFP遺伝子封入L粒子を尾静脈より注射して（局注でなく経静脈的な投与を行うことで，遺伝子封

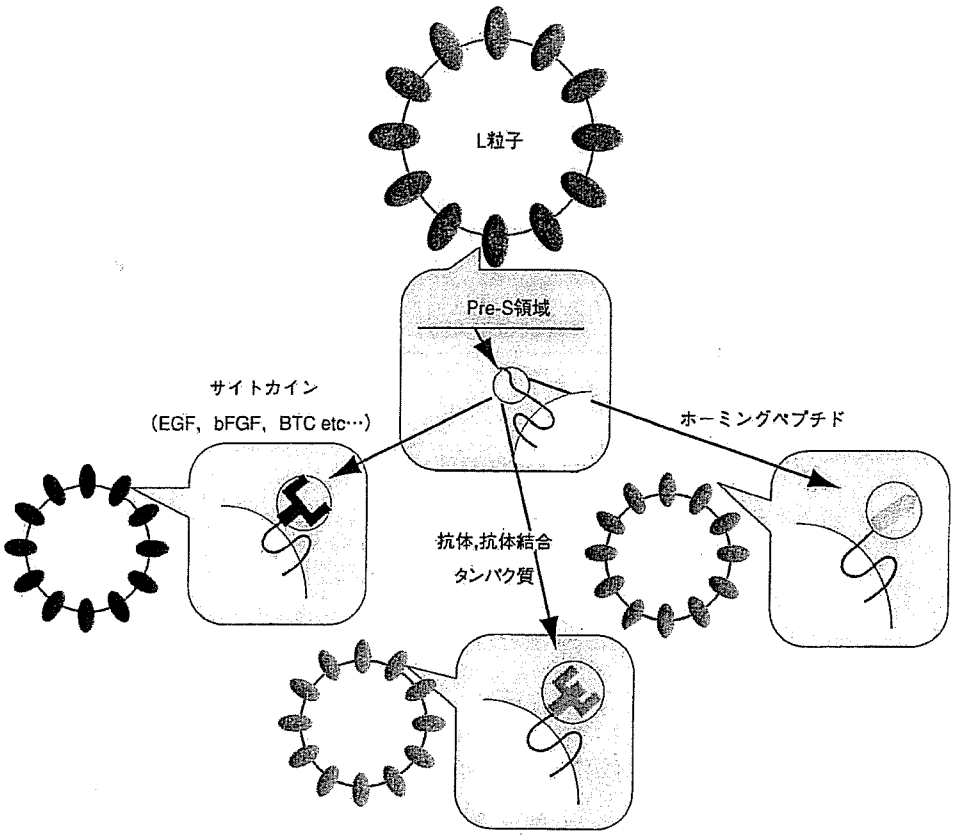

図４●中空バイオナノ粒子のリターゲッティング

Lタンパク質のPre-S領域にある肝細胞認識領域を，サイトカイン，抗体，抗体結合タンパク質，ホーミングペプチドに置換することで中空バイオナノ粒子の標的特異性を置換（リターゲッティング）できる

入L粒子の標的化能力を明らかにするため），L粒子が移植ヒト肝細胞がんに特異的に遺伝子導入できるかを蛍光観察により判定した．投与2週間後に，腫瘍を切除して組織内の蛍光を観察すると，ヒト肝細胞がん由来の組織内においてGFPに由来する緑色蛍光が観察された．一方，移植した大腸がん組織や，ヌードマウスの正常組織では緑色蛍光は一切観察されなかった．したがって，中空バイオナノ粒子は生体内で，HBVのようにヒト肝細胞を特異的に遺伝子導入できることが明らかとなった[11)-13)]．また，移植した腫瘍は本来の肝臓の存在位置とは別の部分に存在するにもかかわらず，標的化できたことから，遠方からの能動的な標的化が可能であると考えられる．

さらに中空バイオナノ粒子は，薬剤[11)]やタンパク質[15)]の肝細胞特異的な導入も可能であることが明らかになっている

4．中空バイオナノ粒子のがん遺伝子治療への応用

中空バイオナノ粒子のピンポイント遺伝子デリバリーへの有効性が明らかとなったため，肝臓がんの遺伝子治療への応用をめざして，チミジンキナーゼ遺伝子封入L粒子の抗腫瘍性効果の検討を行った．モデル系としては，ヒト肝細

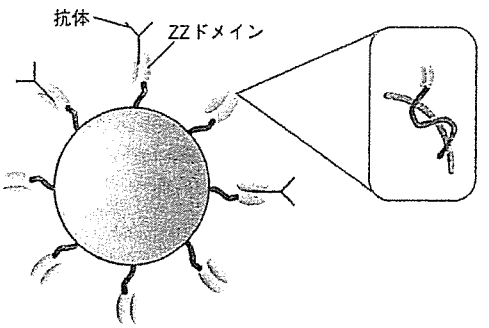

図5●ZZ提示粒子による，抗体の特異性に応じたターゲッティング

Lタンパク質のPre-S領域にある肝細胞認識領域を，抗体のFc領域と結合するProtein A由来のZZタンパク質と置換したZZ提示粒子．ZZが抗体を結合するため抗体の特異性に応じたターゲッティングができる

胞がん由来の細胞株NuEを皮下に移植させたヌードマウスを用いた．バイオナノ粒子に，チミジンキナーゼを発現するプラスミドを封入し，尾静脈より注射した後に，プロドラッグであるガンシクロビルを投与した．その結果，チミジンキナーゼ発現プラスミドを導入した群では，対照群に比して有意にがん細胞の増殖が著しく抑制されることが明らかとなった[16]．まだ初歩的な検討段階であるが，今後，より有効な治療用遺伝子をピンポイントデリバリーすることで，より有効ながん遺伝子治療が確立できるものと期待される．

5. 中空バイオナノ粒子のリターゲッティング

中空バイオナノ粒子を構成するLタンパク質においては，肝臓細胞を分子認識する部位がpre-S1領域にあることがわかっている．したがってこの肝細胞認識部位の適当な領域を削除して，そこに他の臓器を特異的に認識する分子を挿入することで，任意の臓器に遺伝子や薬剤を標的化することが可能となると期待される（リターゲッティングという）．図4には，各種のサイトカイン，抗体分子，抗体結合分子（各種細胞や組織に特異的な抗体を粒子に結合できる）を用いたリターゲッティングを示すが，われわれはすでに代表的な系で成功している．例えば図5には，抗体結合リガンドZZ（Protein AのBドメインから作られたリガンドで，分子量14,000程度）を提示した粒子の概念図を示す．このZZ提示粒子は抗体を結合できるため，抗体の特異性に応じて，目的の細胞に薬剤や遺伝子を導入できることが明らかになっている．さらに最近，短いペプチドでも細胞や組織特異性をもつことが示された（ホーミングペプチドと呼ばれている）ことから[17]，その利用も有望である．特異性を示す「荷札」となる新しいホーミングペプチドを効率よく探索するうえでは，最近大きな進展を見せているコンビナトリアル・バイオエンジニアリングの手法がきわめて有効であろう[18]．

Lタンパク質をリターゲッティングした中空バイオナノ粒子を用いれば，望みの臓器・組織へのピンポイントな遺伝子の送達ができると期待される．特にがん遺伝子治療を考えた場合，がん細胞のみを正常な細胞と区別して特異的に遺伝子デリバリーできるホーミングペプチドなどの分子を提示した中空バイオナノ粒子が利用できれば，その有用性はきわめて大きいと期待される．現在のがん治療を難しくしている点に，周辺・遠隔臓器への転移の問題がある．中空バイオナノ粒子の高い標的性を利用すれば，多臓器への転移がんを網羅的に治療できると期待される．

おわりに

中空バイオナノ粒子は，ウイルス表面抗原タンパク質の自己組織化によって形成される中空ナノ粒子を利用する，という新しい概念による革新的なナノキャリアである．中空バイオナノ粒子を用いた治療を従来技術と比較すると，中空バイオナノ粒子はウイルスと同様な高い遺伝子導入効率を示すとともに，人工系であること

からリポソームや合成高分子ミセルと同様に安全であり，両者の良い点を併せ持つといえる．量産化に関しても，すでに実績をもつ．さらに高い標的化能力をもつことから，遺伝子治療において待ち望まれていたキャリアであるといえる．ただ問題点として，中空バイオナノ粒子の免疫原性や，ウイルス感染などでB型肝炎ウイルスに対する抗体をすでにもっている人への中空バイオナノ粒子の投与が難しいことがあったが，HBVのエスケープミュータントを模倣する形で免疫系に認識されないステルス粒子を創生することを試み，有望な結果を得ている．このようなことから，われわれは中空バイオナノ粒子に関する基礎的な研究に加えて，その実用化に向けた研究開発についても大学発ベンチャー株式会社ビークル（本社：岡山市：http://www.beacle.com）を設立して進めている．

参考文献

1）Verma, I. M. et al.：Nature, 389：239-242, 1997
2）Marshall, E.：298：34-35, 2002
3）Savulescu, J.：J. Med. Ethics, 27：148-150, 2001
4）Gao, X. & Huang, L.：Gene Ther., 2：710-722, 1995
5）Neurath, A. R. et al.：Cell, 46：429-436, 1986
6）Le, S. J. et al.：J. Virol., 73：2052-2057, 1999
7）De, M. S. et al.：J. Viral. Hepat., 4：145-153, 1997
8）Kuroda, S. et al.：J. Biol. Chem., 267：1953-1961, 1992
9）Yamada, T. et al.：Vaccine, 19：3154-3163, 2001
10）Shishido, T. et al.：Appl. Microbiol. Biotechnol., in press
11）Yamada, T. et al.：Nature Biotechnol., 21：885-890, 2003
12）Lawrence, D.：Lancet, 362：48, 2003
13）Russel, S. J.：Nature Biotechnol., 21：872-873, 2003
14）鄭周姫　ほか：化学工学会第37回秋季大会，E2072, 2005
15）Yu, D. et al.：FEBS Journal, 272：3651-3660, 2005
16）Iwasaki, Y. et al.：Cancer Gene Therapy, in press
17）Arap, W. et al.：Nature Medicine, 8：121-127, 2002
18）「コンビナトリアル・バイオエンジニアリング」（植田充美，近藤昭彦／編），化学同人，2003

近藤昭彦（Akihiko Kondo）

神戸大学工学部応用化学科教授．
1983年京都大学工学部卒，1988年工学博士取得，1988年九州工業大学工学部講師，1993年助教授，1995年神戸大学助教授，2003年より現職．
専門：バイオナノキャリアによるドラッグ・遺伝子デリバリーシステムの開発，機能性磁性微粒子材料のバイオ分野への応用，バイオマスからのバイオ燃料・化学品の生産，などの研究を行っている．

黒田俊一（Shun-ichi Kuroda）

大阪大学産業科学研究所助教授．

谷澤克行（Katsuyuki Tanizawa）

大阪大学産業科学研究所教授．

妹尾昌治（Masaharu Seno）

岡山大学大学院自然科学研究科助教授．

上田政和（Masakazu Ueda）

慶應義塾大学医学部助教授．

Anti-tumor effect in an *in vivo* model by human-derived pancreatic RNase with basic fibroblast growth factor insertional fusion protein through antiangiogenic properties

Hiroshi Yagi,[1] Masakazu Ueda,[1,4] Hiromitsu Jinno,[1] Koichi Aiura,[1] Shuji Mikami,[2] Hiroko Tada,[3] Masaharu Seno,[3] Hidenori Yamada[3] and Masaki Kitajima[1]

Departments of [1]Surgery, and [2]Pathology, Keio University School of Medicine, Tokyo; [3]Department of Bioscience and Biotechnology, Faculty of Engineering, Graduate School of Natural Science and Technology, Okayama University, Okayama, Japan

(Received July 13, 2006/Revised August 23, 2006/Accepted August 27, 2006/Online publication October 18, 2006)

It is thought that the export of angiogenic fibroblast growth factors (FGF) from tumors may be involved in the onset of tumor angiogenesis. To create a new active targeting drug that inhibits the tumor angiogenic process without toxicities to normal cells, human basic FGF (h-bFGF) was inserted genetically into the Gly89 position of cross-linked RNase1 (the ribonuclease inhibitor protein [RI] binding site of cross-linked human pancreatic RNase) to prevent stereospecific binding to RI. The resultant insertional-fusion protein (CL-RFN89) was active both as h-bFGF and as RNase1. Furthermore, it acquired an additional ability of evading RI through steric blockade of RI binding caused by the fused h-bFGF domain. In the present study, the effect of the resultant protein, CL-RFN89, on the antitumor response though its antiangiogenic properties was investigated in an *in vivo* model. Continuous systemic treatment with CL-RFN89 significantly inhibited the growth of human A431 squamous cell carcinomas *in vivo*. Seven days of treatment with CL-RFN89 resulted in a 58.2% inhibition of tumor growth compared with control mice ($P < 0.0001$). Furthermore, immunohistochemistry using a rat antimouse CD31 antibody showed that treatment with CL-RFN89 reduced tumor vascularization. These findings identify CL-RFN89 as a potent systemic inhibitor of tumor growth as a result of its antiangiogenic properties. This protein appears to be a new systemic antitumor agent. (*Cancer Sci* 2006; 97: 1315–1320)

Improvement of cytotoxic agents specific to cancer cells or other cells causing proliferative diseases is one of the goals of targeted chemotherapy. Such cells often express surface receptors or other molecules distinguishing them from the surrounding normal cells. In this regard, many immunotoxins have been developed that exploit this difference. Immunotoxins are defined as proteins containing an antibody (or a ligand) and a toxin.[1,2] The antibody moiety or ligand specific for a cell surface molecule delivers the toxin to the target cells. Plant and bacterial toxins have been the most intensively studied moieties. These toxins are enzymes that catalytically abolish protein synthesis when they translocate into the cytosol. However, clinical applications are still limited owing to the inherent toxicities of these substances to normal cells, in addition to their immunogenicity. Distinct targeting specificity and humanization of immunotoxins are needed to overcome these difficulties.

There is increasing evidence that malignant tumor growth and progression are dependent on the induction of tumor angiogenesis,[3–5] and clinical studies have revealed that high vessel density often correlates with poor prognosis.[6] Angiogenesis is regulated by a fine balance between inducers and inhibitors of this process (angiogenic and angiostatic factors, respectively).[7] For tumor metastasis, it is necessary for the neoplasm to grow beyond 1–2 mm in diameter.[8] Therefore, inhibition of the angiogenic process has become one of the most promising strategies for the treatment of malignant neoplasms.

Basic fibroblast growth factor (bFGF) is a prototype member of a family of structurally related growth factors that exert important pleiotropic effects on cell differentiation and organ development *in vitro* and *in vivo*.[9–11] bFGF plays an important role in many of these processes and represents one of the most potent inducers of angiogenesis known, functioning both as an autocrine and a paracrine factor to stimulate vascular endothelial cell proliferation and migration, and induction of the expression of specific proteases, growth factors and integrins involved in angiogenesis.[12–14] As overexpression of fibroblast growth factor (FGF) receptors possibly correlates with the malignancy of tumors and bFGF is proposed to support autocrine growth of melanoma cells,[15] the receptors are potential targets for melanoma therapy.[16] In fact, chemical conjugates or fusion proteins between bFGF and saporin, a ribosome-inactivating protein isolated from the plant *Saponaria officinalis*, have been developed that show growth inhibitory effects on cells expressing FGF receptors.[17–19]

In an attempt to make fusion proteins safer for clinical use, we and others have introduced the use of mammalian enzymes such as ribonucleases (RNases) instead of bacterial toxins.[20–22] RNases constitute a large superfamily across many species.[23] Some members are cytotoxic and have antitumor activity. Mammalian RNase is non-toxic to cultured cells and can be substituted for plant or bacterial toxins as an immunotoxin.[24] Bovine pancreatic RNase A chemically conjugated to human transferrin and to antibodies to the transferrin receptor became cytotoxic specifically to those cells bearing the transferrin receptor.[20] It was shown that bovine pancreatic RNase A can selectively eliminate squamous carcinoma cells overexpressing epidermal growth factor receptors *in vitro* when chemically coupled to human epidermal growth factor (hEGF).[25] The availability of recombinant human pancreatic RNase (RNase1), the human homolog of bovine pancreatic RNase A that we cloned from human pancreas,[26] enabled us to construct a totally human chemical conjugate of hEGF and RNase1, which was found to be equally potent *in vitro*.[21] In order to stabilize RNase1 by the introduction of an intramolecular cross link, a mutant protein (4–118 CL RNase1), in which Arg4 and Val118 are replaced with cysteine residues and linked by a disulfide bond, was designed and expressed in *Escherichia coli* as inclusion bodies.[27] However, a previous study showed that in the cytosol, RNase encounters the ribonuclease inhibitor protein (RI) and is inactivated by

[4]To whom correspondence should be addressed. E-mail: m_ueda@sc.itc.keio.ac.jp

doi: 10.1111/j.1349-7006.2006.00336.x

forming a tight complex that prevents RNA substrates from entering the active sites of the enzyme.[28]

Several kinds of hybrid proteins have been constructed to produce bifunctional proteins and utilized as tools such as detectors for biological molecules. Generally, these hybrid proteins have been built by end-to-end fusion (tandem-fusion) of two genes of the component proteins. Previously, Futami *et al.* constructed cytotoxic RNase by fusing human bFGF (h-bFGF) to the C-terminus of RNase1.[29] The resultant tandem-fusion protein inhibited the growth of malignant cells expressing high levels of cell surface FGF receptor. However, its activity was still weak (IC_{50} [protein concentration that promotes a 50% inhibition of cell growth] > 1 μM), which could be due to incomplete inactivation by RI. Recently, Hoshimoto *et al.* had made des. 1–7 RNase1, which is an RNase1 variant created by mutagenesis of the DNA sequence encoding the RNase inhibitor binding site and fusion of the DNA with hEGF DNA.[30] The new protein expressed from the genetically altered DNA had reduced RNase activity but exhibited an even greater reduction in its affinity to bind RNase inhibitor. However, the protein was unstable.

The alternative is to insert the second protein (the insert protein) into the middle of the sequence of the host protein in-frame. This new mode of gene fusion (insertional-fusion) is expected to give an additional configuration between the two component domains and to make it possible to create the hybrid protein with the ideal 3-dimensional structure for new functions.[31] To create a new active targeting drug that inhibits the tumor angiogenic process without toxicities to normal cells, h-bFGF was inserted genetically into Gly89 of cross-linked RNase1 (the RI binding site of cross-linked RNase1) to prevent its stereo-specific binding to RI. The resultant insertional-fusion protein (CL-RFN89) was active both as h-bFGF and as RNase1. Furthermore, it acquired an additional ability of evading RI through steric blockade of RI-binding caused by the fused h-bFGF domain. CL-RFN89 retained more than 85% of its activity even in the presence of a 200-fold molar excess of RI and showed growth inhibitory effects on mouse B16/BL6 melanoma cells,[31] which express both bFGF and high-affinity FGF receptor.[32] Subsequently, tumor angiogenesis, which is mediated and promoted by the interaction of bFGF and the FGF receptor, was suppressed by this fusion protein.[33]

In the present study, the effect of CL-RFN89 on the antitumor response though its antiangiogenic properties was investigated in an *in vivo* model. Continuous systemic treatment with CL-RFN89 significantly inhibited the growth of human A431 squamous cell carcinomas (SCC) *in vivo*. Seven days of treatment with CL-RFN89 resulted in a 58.2% inhibition of tumor growth compared with control mice ($P < 0.0001$). Furthermore, immunohistochemistry using a rat antimouse CD31 antibody showed that the treatment with CL-RFN89 reduced tumor vascularization. These findings identify CL-RFN89 as a potent systemic inhibitor of tumor growth as a result of its antiangiogenic properties.

Materials and Methods

Cell lines. A431 SCC cells procured form Riken (Saitama, Japan) were maintained in Dulbecco's Modified Eagles Medium containing 10% fetal bovine serum. All the cells were cultured in an atmosphere of 5% CO_2 at 37°C.

Animals. Four-week-old female BALB/c (nu/nμ) mice were obtained from CLEA Japan (Tokyo, Japan). The animals were housed in an airconditioned room at 22–23°C, with free access to food and water.

Construction of CL-RFN89. Construction and purification of the insertional fusion protein CL-RFN89 has been described previously.[31] Briefly, recombinant human 4–118 cross-linked RNase1 (CL-RNase1) and human bFGF (147 amino acid form) were purified from *Escherichia coli*.[29,34] A cDNA encoding bFGF (19–146) (N-terminal 18-residue truncated form of bFGF) was amplified by polymerase chain reaction. A *Sac*II site was introduced at Gly89 of the CL-RNase1 cDNA and the cDNA was inserted into a CL-RNase1 expression vector. The resultant plasmid was cleaved with *Sac*II and ligated in-frame with the *Sac*II fragment of bFGF (19–146) to construct the expression vectors for insertional-fusion proteins.[31] All of the insertional-fusion proteins were expressed as inclusion bodies in *E. coli*, solubilized, refolded and purified as described previously.[29,31,34] The estimated molecular weight was 28.94 kDa. The purified proteins were concentrated by ultrafiltration with an Ultrafree-4 centrifugal filter (Biomax-5K NMWL; Millipore, Bedford, MA, USA). Protein concentrations were determined by ultraviolet spectroscopy as described previously.[35]

***In vivo* tumorigenesis assays.** Four-week-old, female BALB/c (nu/nμ) mice were injected intradermally with human A431 SCC cells (5×10^6) on the right flank. One day after tumor cell inoculation, mice were injected intraperitoneally with 50 μM (200 μL; 0.3 mg) of CL-RFN89, 50 μM (200 μL; 0.2 mg) of bFGF and 200 μL of phosphate-buffered saline (PBS). After injection, ALZET Osmotic Pumps (Durect, Cupertino, CA, USA) were placed subcutaneously in the left flank of each mouse (Fig. 1b). The pumps contained 200 μL (0.3 mg) of CL-RFN89 (50 μM), or 200 μL (0.2 mg) of bFGF (50 μM) alone, or 200 μL of PBS (control). The pumps released the solutions continually for 1 week (approximately 10 μM per day). There were eight mice each in the CL-RNase1 and PBS groups and four mice in the bFGF group. The smallest and largest tumor diameters were measured every day and tumor volumes were calculated using the following formula:

$$(4/3) \times \pi \times (1/2 \times \text{smallest diameter})^2 \times 1/2 \times \text{largest diameter}.$$

All tumors were resected and their weights measured.

Tumor data were analyzed by repeated measure one-way ANOVA followed by Fisher's least significant difference for multicomparison, in which each value was compared with the control value. StatView software was used for statistical calculations (Abacus Concepts, Berkeley, CA, USA).

Immunohistochemistry. For histological analysis, tumors were harvested from three additional animals per treatment group. Eleven days after the start of therapy and at the end of the observation period, they were removed, frozen rapidly and stored at −80°C. Frozen tissues were embedded in Optimal Cutting Temperature (OCT) compound and prepared by hexane quenching. After this, these frozen tumor tissues were cut into serial thin sections (4 μm) in the cryostat (−20°C). General tissue morphology was visualized and photographed with a camera (Olympus DP-50 CUl; Olympus Optical, Tokyo, Japan) mounted on a microscope (Olympus BX51 TF; Olympus Optical). Staining was carried out at room temperature throughout using the Rat ABC Staining System (SC-2019; Santa Cruz Biotechnology, Santa Cruz, CA, USA). The sections were then incubated overnight at 4°C in the presence of a rat antimouse CD31 antibody (dilution 1:100; Fitzgerald Industries International, Concord, MA, USA) (Fig. 2a1–c1). Counterstaining was carried out with Carazzi's hematoxylin (Fig. 2a2–c2) and the corresponding frozen tumor sections were also stained with hematoxylin and eosin using standard techniques (Fig. 2a3–c3).

Microvessel density was determined by computer-assisted analysis. For the analysis of tumor vessels, CD31-stained sections were imaged with a digital camera at ×100 magnification and morphometric analysis was carried out using Adobe Photoshop 7.0 (Adobe Systems, San Jose CA, USA) and Image J (Research Services Branch of the National Institute of Mental Health, Bethesda, MD, USA). At least three different fields in each section were examined for relative area occupied by tumor blood vessels, as described previously.[36] The repeated measure

doi: 10.1111/j.1349-7006.2006.00336.x

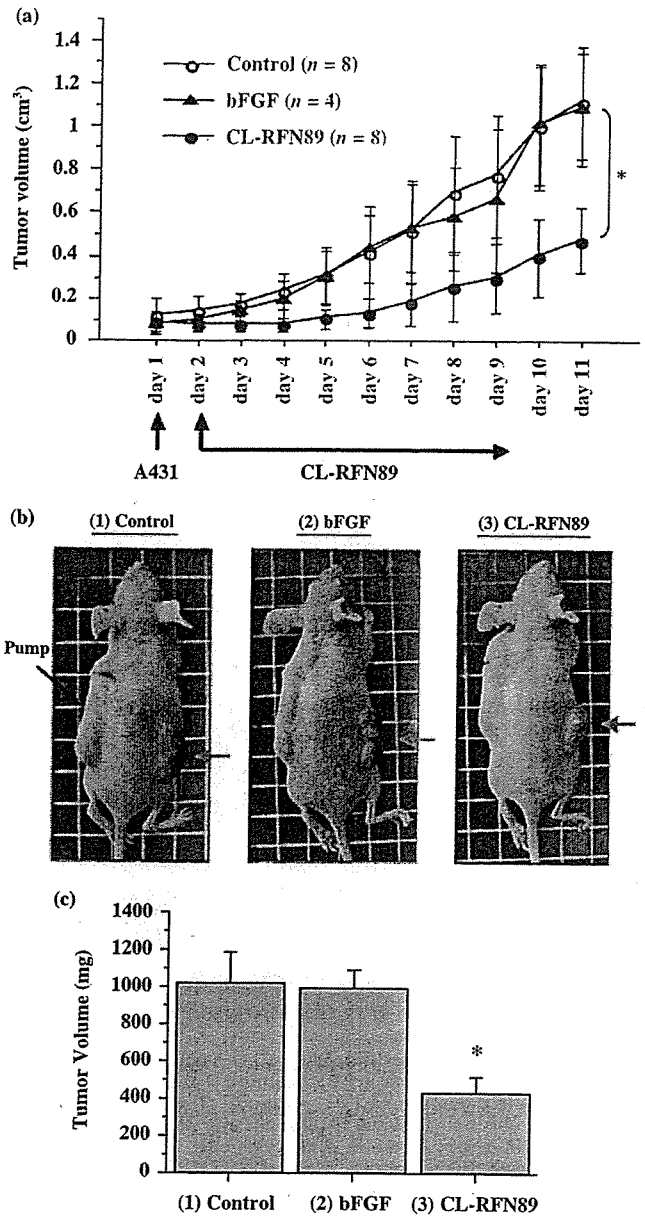

Fig. 1. Systemic therapy with CL-RFN89 inhibits tumor growth of A431 *in vivo*. One day after tumor cell inoculation, mice were injected intraperitoneally with CL-RFN89, basic fibroblast growth factor (bFGF) and phosphate-buffered saline (PBS). The pumps placed in each mouse after injection contained CL-RFN89, bFGF alone or PBS (control), and they released the liquids continually for 1 week. (a) Systemic treatment with CL-RFN89 significantly inhibited human A431 tumor growth compared with control mice (*$P = 0.0003$). Error bars show the SD. (b) The representative pictures show retarded tumor growth after CL-RFN89 treatment (3) compared with PBS-control treatment (1) and bFGF treatment (2). (c) The final mean weights of the tumors were 1018.8 ± 164.7 mg ($n = 8$) (1), 993.0 ± 96.5 mg ($n = 4$) (2) and 426.3 ± 86.3 mg ($n = 8$) (3). CL-RFN89 treatment (3) showed 58.2% inhibition of tumor growth compared with control-treated mice (1) (*$P < 0.0001$). Error bars show the SD.

one-way ANOVA followed by Fisher's least significant difference for multicomparison was used for statistical analysis; each value was compared with the control value obtained using StatView.

Results

Inhibition of *in vivo* tumor growth by systemic treatment with CL-RFN89. We first investigated whether recombinant CL-RFN89 affects tumor angiogenesis and malignant tumor growth *in vivo* with systemic delivery of CL-RFN89 by intraperitoneal injection into tumor-bearing mice. We took this approach because local intratumor or peritumor injection of antiangiogenic drugs would probably not be feasible in most human patients. A431 SCC cells were implanted intradermally into immunosuppressed mice. CL-RFN89 and bFGF treatments were initiated after 1 day and continued by osmotic pump. Mice implanted with A431 SCC cells that were injected with PBS served as a negative control. Systemic treatment with CL-RFN89 significantly inhibited *in vivo* tumor growth ($P = 0.0003$) (Fig. 1a). Seven days of treatment with CL-RFN89 resulted in a significant change; the final mean tumor weights were 1018.8 ± 164.7X mg (control) and 426.3 ± 86.3X mg (CL-RFN89), corresponding to a 58.2% inhibition of tumor growth compared with control mice ($P < 0.0001$). No inhibition of tumor growth was observed by treatment with bFGF alone at a dose that was equivalent to the dose of bFGF the mice received with CL-RFN89. The tumor volumes after treatment of bFGF alone were significantly larger compared with those from mice treated with CL-RFN89 ($P < 0.0001$); the final mean tumor weight was 993.0 ± 96.5 mg for bFGF. There was no statistically significant difference in tumor growth between mice treated with PBS and mice treated with bFGF alone (Fig. 1b,c).

All therapies were well tolerated by the animals. No differences in bodyweight or behavior were observed between the treatment groups. All animals survived until the end of the observation period unless killed. Furthermore, histology of the hematoxylin–eosin-stained sections from organs including liver, spleen, kidney, lung and heart did not reveal therapy-related toxicity.

Systemic treatment with CL-RFN89 inhibits tumor angiogenesis. We next investigated whether systemic treatment with recombinant CL-RFN89 could also inhibit bFGF-driven angiogenesis *in vivo*, as assessed by the *in vivo* tumorigenesis assays. Control and bFGF-treated mice bearing A431 SCC tumors showed tumor vasculature with remarkable heterogeneity in lumen diameters and with numerous large-caliber vessels throughout the viable parts of the tumors, assessed by analysis of CD31-positive vessels (Fig. 2a,b). In contrast, there was less tumor angiogenesis in mice treated with CL-RFN89, characterized by comparatively more homogenous small-caliber vessels (Fig. 2c). Computer-assisted image analysis of CD31-positive vessels indicated that the inhibition of angiogenesis with CL-RFN89 caused a further decrease in total vascular area to values 95% lower than those measured in control and bFGF-treated tumors ($P < 0.0001$) (Fig. 3).

Discussion

In the present study, systemic inhibition of tumor growth was evaluated in A431 SCC tumor-bearing mice using CL-RFN89, a novel insertional fusion protein consisting of h-bFGF inserted into the Gly89 position of cross-linked RNase1, which was expected to inhibit RNase inhibitor interreaction. Futami *et al.* showed that cell lines expressing FGF receptors were inhibited in their growth by micromolar concentrations of RNase1–h-bFGF fusion proteins.[29] In contrast, no growth inhibition was observed in A431 cells that did not express FGF receptors.

Tumor-bearing mice received intraperitoneal injections of 50 μM of CL-RFN89 (50-fold concentration of that used in the *in vitro* assay) and subcutaneous continuous injection using an osmotic pump for 7 days with 10 μM (10-fold concentration of that used in the *in vitro* assay) of CL-RFN89 each day. It was found that CL-RFN89 significantly inhibited the growth of

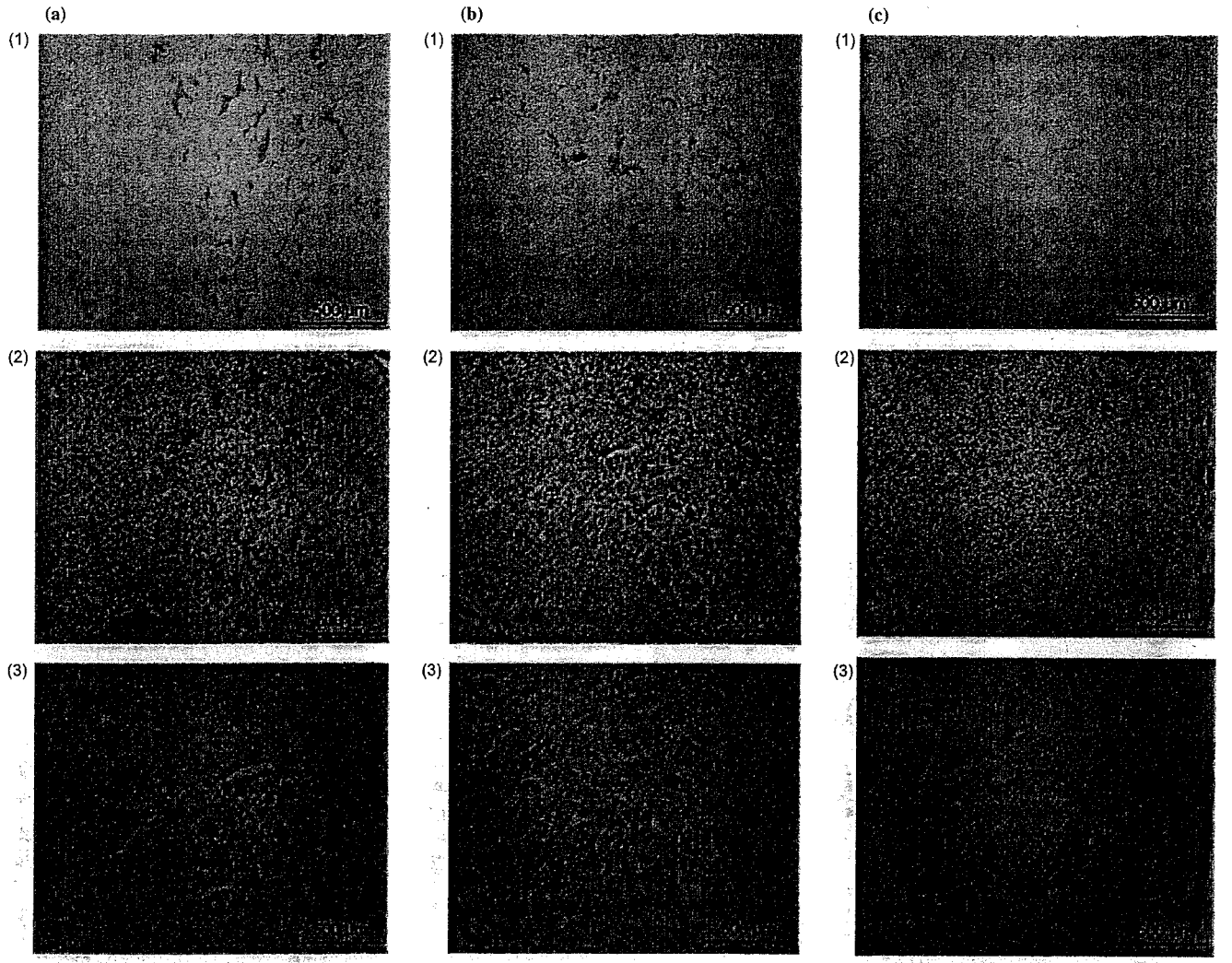

Fig. 2. Immunohistochemistry of A431 tumors. Tumor cell proliferation and microvessel density were assessed by CD31 immunostaining of A431 tumors excised on day 11 after the start of therapy. Mice were treated with phosphate-buffered saline (PBS) (control), basic fibroblast growth factor (bFGF) alone or CL-RFN89 as shown in Fig. 1. (1) The sections were incubated in the presence of a CD31 antibody. (2) Counterstaining was carried out using Carazzi's hematoxylin. (3) Corresponding frozen tumor sections were also stained with hematoxylin and eosin. (a) Control and (b) bFGF-treated A431 squamous cell carcinoma showed remarkable heterogeneity in lumen diameter with numerous large-caliber vessels throughout the viable parts of the tumors, as assessed by analysis of CD31-positive vessels. (c) In contrast, the extent of tumor angiogenesis in tumors of mice treated with CL-RFN89 was less pronounced and was characterized by more homogenous small-caliber vessels.

A431 (58%). In contrast, tumors that were treated with an equivalent dose of h-bFGF as CL-RFN89 showed no significant difference in volume compared with the tumors from mice treated with PBS (control). Also, our results suggested that h-bFGF itself had no direct antitumor activity for A431 tumors *in vivo*. However, computer-assisted analysis of tumor vessels stained with a rat antimouse CD31 antibody revealed a significant reduction of tumor vascularization after treatment with CL-RFN89.

With regard to these results, there are a number of questions to be clarified as to how this new insertional-fusion protein, CL-RFN89, acts as an antitumor agent. CL-RFN89 binds to FGF receptors on the surface of cells through the specificity of h-bFGF. It is then internalized into the cytosol where RNaseI exterts its cytotoxic effects. The mechanism of ribonuclease-mediated cytotoxicity is not known in detail.[37–39] To demonstrate internalization of RNaseI into the cytosol, Futami *et al.* used fluorescence-labeled RNaseI derivatives.[40] Tada *et al.* then showed IC_{50} values of wild-type RNaseI, tandem-fusion RNaseI–h-bFGF and CL-RFN89 in terms of their growth inhibitory effect on mouse melanoma B16/BL6 cells,[31] which express high-affinity FGF receptor.[32] Wild-type RNaseI activity was almost completely cancelled in the presence of RI and its IC_{50} value could not be detected. In contrast, both of the fusion proteins inhibited the growth of B16/BL6 melanoma cells, and the IC_{50} value of CL-RFN89 was five-fold lower then that of tandem-fusion RNaseI–h-bFGF. These results suggested that the cytotoxicity of CL-RFN89 was caused not by internalization of RNaseI itself but by internalization of CL-RFN89 with an evasion of RI binding through steric blockade after an interaction on the plasma membrane of a target cell.

In addition, Hayashida *et al.* demonstrated that CL-RFN89 worked specifically by intervention of bFGF–FGF receptor interaction on A431 tumor.[33] Using fluorescence-labeled protein they showed that CL-RFN89 could adhere to the surface of human umbilical vein endothelial cells (HUVEC). However, in the presence of an excess amount of unlabeled h-bFGF, no adhesion or uptake of CL-RFN89 occurred. This means that the excess bFGF occupies the FGF receptors and competitively

doi: 10.1111/j.1349-7006.2006.00336.x

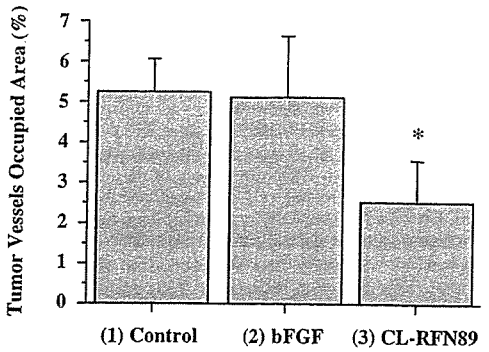

Fig. 3. Computer-assisted image analysis of CD31-positive vessels indicated that the inhibition of angiogenesis with CL-RFN89 ($n = 11$) caused a further decrease in total vascular area to values 95% lower ($^*P < 0.0001$) than those measured in control ($n = 11$) and basic fibroblast growth factor (bFGF)-treated tumors ($n = 12$). Error bars show the SD.

prevents CL-RFN89 from binding to the cells, which suggests that the binding of the protein to HUVEC is FGF receptor dependent. Also, they showed that CL-RFN89 inhibited the growth of HUVEC in a dose-dependent manner. These previous results showed that CL-RFN89 was active both as h-bFGF and as RNase1.

There is one question remaining, and that is whether the inhibition of A431 tumor growth is based solely on the antiangiogenic property of the molecule. Tumor growth and metastasis are dependent on angiogenesis.[41] A tumor must continuously stimulate the growth of new capillary blood vessels for it to grow. Furthermore, the new blood vessels embedded in a tumor provide a gateway for tumor cells to enter the circulation and to metastasize to distant sites, such as liver, lung or bone. There are several angiogenic polypeptides such as bFGF, acidic fibroblast growth factor, vascular endothelial growth factor, transforming growth factor and angiogenin, with several reports describing how neovascularization of tumors is part of the genetically based tumor progression and bFGF is strongly correlated with this mode of vascularization.[7,8,42] Hori *et al.* demonstrated that solid tumor growth could be suppressed by inactivation of bFGF alone *in vivo*.[43] They prepared anti-bFGF neutralizing monoclonal antibodies as a bFGF inhibitor and showed that it could suppress tumor angiogenesis. This result suggests that bFGF is one of the most important factors in tumor angiogenesis. In addition, Hayashida *et al.* showed that CL-RFN89 had no direct cytotoxicity against A431 cells *in vitro*, but had an antiangiogeneic response *in vitro* and *in vivo* using HUVEC and in the mouse dorsal air sac assay, which suggested that CL-RFN89 is functioned as an anti-bFGF agent.[33] In the present study, the computer-assisted analysis showed a significant reduction in tumor vascularization *in vivo* after treatment with CL-RFN89. Both the previous results and our results did not completely deny the possibility of indirect action with respect to antiangiogenic activity on progenitor cells, but supported the view that the most important influence was the inhibitory effect of CL-RFN89 in tumor growth by suppression of angiogenesis, and that the effect is exerted through FGF–FGF receptor interactions on cells bearing FGF receptors, such as endothelial cells, with a role in neovascularization.[33]

Though it would be helpful if the *in vivo* distribution of CL-RFN89 was shown, we did not try to visualize it in the present study. This was because we thought that the biological half-life of CL-RFN89 might be less then 24 h, and that when CL-RFN89 accumulated in the cells bearing FGF receptors (such as endothelial cells) they would become apoptotic. It therefore seemed difficult to visualize the accumulation of this protein.

Compared with other immunotoxins, this new insertional-fusion protein, CL-RFN89, is expected to be less toxic to humans because the components are human-derived and appear to have a higher stability and RI-evading ability. In support of these statements, this new protein has several important characteristics as follows: (1) it is made from both human RNase and human bFGF; and (2) it is based on a 3-dimensional structural design that allows insertion of bFGF into cross-linked RNase1 at the exact RI-binding site. In addition, the dose of this protein needed for systemic treatment was approximately 50-fold that used in the *in vitro* assay, and was considered an acceptable dose to use *in vivo*. Also, this macromolecular agent would have an advantage compared with other micromolecular drugs. Noguchi *et al.* reported that there was a great difference in the clearance rate between solid tumors and normal tissues in the early phase of accumulation of macromolecules in tumors.[44] They showed that higher molecular weight copolymers had significantly higher tumor accumulation, whereas the lower molecular weight copolymers were cleared rapidly from tumor tissue due to rapid diffusion back into the bloodstream. Also, Dreher *et al.* investigated how molecular weight influenced the accumulation of a model macromolecular drug carrier in tumors using dextran.[45] They concluded that increasing the molecular weight of dextran significantly reduced its tumor vascular permeability, and dextrans of 40 and 70 kDa had the highest accumulation in solid tumors but were largely concentrated near the vascular surface. These results suggest that macromolecular drugs such as CL-RFN89 have higher accumulation in targeted tumors and lower toxicity to normal cells than micromolecular drugs such as the tyrosine kinase inhibitors.

These findings identify CL-RFN89 as a potent systemic inhibitor of tumor growth as a result of its antiangiogenic properties. This protein appears to be a new systemic antitumor agent.

Acknowledgments

The authors thank Mrs Yuki Nakamura and Mr Toshihide Muramatsu from the laboratory of Keio University School of Medicine and Mr Yasushi Saze, Mrs Mariko Koshiba and Ms Kazuko Nakayama from Hino Municipal Hospital for their technical support and helpful discussions. This research was supported by a Ministry of Education, Culture, Sports, Science and Technology Grant-in-Aid for Scientific Research (B) and a Grant-in-Aid for the 21st Century Center of Excellence (COE) Program entitled 'Establishment of individualized cancer therapy based on comprehensive development of minimally invasive and innovative therapeutic methods (Keio University)'.

References

1 Lappi DA, Baird A. Mitotoxins: growth factor-targeted cytotoxic molecules. *Prog Growth Factor Res* 1990; **2**: 223–36.
2 Pastan II, Kreitman RJ. Immunotoxins for targeted cancer therapy. *Adv Drug Deliv Rev* 1998; **31**: 53–88.
3 Folkman J. New perspectives in clinical oncology from angiogenesis research. *Eur J Cancer* 1996; **32**: 2534–9.
4 Hanahan D, Folkman J. Patterns and emerging mechanisms of the angiogenic switch during tumorigenesis. *Cell* 1996; **86**: 353–64.
5 Hanahan D, Christofori G, Naik P, Arbeit J. Transgenic mouse models of tumour angiogenesis: the angiogenic switch, its molecular controls, and prospects for preclinical therapeutic models. *Eur J Cancer* 1996; **32**: 2386–93.
6 Weidner N, Folkman J. Tumoral vascularity as a prognostic factor in cancer. *Important Adv Oncol* 1996: 67–190.
7 Risau W. Mechanisms of angiogenesis. *Nature* 1997; **386**: 671–4.
8 Folkman J, Shing Y. Angiogenesis. *J Biol Chem* 1992; **267**: 10931–4.
9 Klagsbrun M. The fibroblast growth factor family: Structural and biological properties. *Prog Growth Factor Res* 1989; **1**: 207–35.
10 Mason I. The ins and outs of fibroblast growth factors. *Cell* 1994; **78**: 547–52.
11 Bikfalvi A, Klein S, Pintucci G, Rifkin D. Biological roles of fibroblast growth factor-2. *Endocr Rev* 1997; **18**: 26–45.

12 Beck L, D'Amore P. Vascular development: Cellular and molecular regulation. *FASEB J* 1997; **11**: 365–73.
13 Seghezzi G, Patel S, Ren C *et al.* Fibroblast growth factor-2 (FGF-2) induces vascular endothelial growth factor (VEGF) expression in the endothelial cells of forming capillaries: An autocrine mechanism contributing to angiogenesis. *J Cell Biol* 1998; **141**: 1659–73.
14 Rusnati M, Tanghetti E, Urbinati C *et al.* Interaction of fibroblast growth factor-2 (FGF-2) with free gangliosides: Biochemical characterization and biological consequences in endothelial cell cultures. *Mol Biol Cell* 1999; **10**: 313–27.
15 Ahmed NU, Ueda M, Ito A, Ohashi A, Funasaka Y, Ichihashi M. Expression of fibroblast growth factor receptors in naevus-cell naevus and malignant melanoma. *Melanoma Res* 1997; **7**: 299–305.
16 Kato J, Wanebo H, Calabresi P, Clark JW. Basic fibroblast growth factor production and growth factor receptors as potential targets for melanoma therapy. *Melanoma Res* 1992; **2**: 13–23.
17 Lappi DA, Maher PA, Martineau D, Baird A. The basic fibroblast growth factor–saporin mitotoxin acts through the basic fibroblast growth factor receptor. *J Cell Physiol* 1991; **147**: 17–26.
18 Lappi DA, Ying W, Barthelemy I *et al.* Expression and activities of a recombinant basic fibroblast growth factor–saporin fusion protein. *J Biol Chem* 1994; **269**: 12552–8.
19 Beitz JG, Davol P, Clark JW *et al.* Antitumor activity of basic fibroblast growth factor–saporin mitotoxin *in vitro* and *in vivo*. *Cancer Res* 1992; **52**: 227–30.
20 Rybak SM, Saxena SK, Ackerman EJ, Youle RJ. Cytotoxic potential of ribonuclease and ribonuclease hybrid proteins. *J Biol Chem* 1991; **266**: 21202–7.
21 Jinno H, Ueda M, Ozawa S *et al.* Epidermal growth factor receptor-dependent cytotoxicity for human squamous carcinoma cell lines of a conjugate composed of human EGF and RNase1. *Life Sci* 1996; **58**: 1901–8.
22 Psarras K, Ueda M, Yamamura T *et al.* Human pancreatic RNase1–human epidermal growth factor fusion: an entirely human 'immunotoxin analog' with cytotoxic properties against squamous cell carcinomas. *Protein Eng* 1998; **11**: 1285–92.
23 Beintema JJ. Introduction: the ribonuclease A superfamily. *Cell Mol Life Sci* 1998; **54**: 763–5.
24 Rybak SM, Pearson JW, Fogler WE *et al.* Enhancement of vincristine cytotoxicity in drug-resistant cells by simultaneous treatment with onconase, an antitumor ribonuclease. *J Natl Cancer Inst* 1996; **88**: 747–53.
25 Jinno H, Ueda M, Ozawa S *et al.* Epidermal growth factor receptor-dependent cytotoxic effect by an EGF-ribonuclease conjugate on human cancer cell lines – a trial for less immunogenic chimeric toxin. *Cancer Chemother Pharmacol* 1996; **38**: 303–8.
26 Futami J, Seno M, Kosaka M, Tada H, Seno S, Yamada H. Recombinant human pancreatic ribonuclease produced in *E. coli*: importance of the amino-terminal sequence. *Biochem Biophys Res Commun* 1995; **216**: 406–13.
27 Futami J, Tada H, Seno M, Ishikami S, Yamada H. Stabilization of human RNase1 by introduction of a disulfide bond between residues 4 and 118. *J Biochem* 2000; **128**: 245–50.
28 Kobe B, Deisenhofer J. Mechanism of ribonuclease inhibition by ribonuclease inhibitor protein based on the crystal structure of its complex with ribonuclease A. *J Mol Biol* 1996; **264**: 1028–43.
29 Futami J, Seno M, Ueda M, Tada H, Yamada H. Inhibition of cell growth by a fused protein of human ribonuclease 1 and human basic fibroblast growth factor. *Protein Eng* 1999; **12**: 1013–19.
30 Hoshimoto S, Ueda M, Jinno H, Kitajima M, Futami J, Seno M. Mechanisms of growth inhibitory effect of RNase–EGF fused proteins against EGFR-overexpressing cells. *Anticancer Res* 2006; **26**: 857–64.
31 Tada H, Onizuka M, Muraki K *et al.* Insertional-fusion of basic fibroblast growth factor endowed ribonuclease 1 with enhanced cytotoxicity by steric blockade of inhibitor interaction. *FEBS Lett* 2004; **568**: 39–43.
32 Blanckaert VD, Schelling ME, Elstad CA, Meadows GG. Differential growth factor production, secretion, and response by high and low metastatic variants of B16BL6 melanoma. *Cancer Res* 1993; **53**: 4075–81.
33 Hayashida T, Ueda M, Aiura K *et al.* Anti-angiogenic effect of an insertional fusion protein of human basic fibroblast growth factor and ribonuclease-1. *Protein Eng Des Sel* 2005; **18**: 321–7.
34 Futami J, Tsushima Y, Tada H, Seno M, Yamada H. Convenient and efficient *in vitro* folding of disulfide-containing globular protein from crude bacterial inclusion bodies. *J Biochem* 2000; **127**: 435–41.
35 Gill SC, von Hippel PH. Calculation of protein extinction coefficients from amino acid sequence data. *Anal Biochem* 1989; **182**: 319–26.
36 Streit M, Stephen AE, Hawighorst T *et al.* Systemic inhibition of tumor growth and angiogenesis by thrombospondin-2 using cell-based antiangiogenic gene therapy. *Cancer Res* 2002; **62**: 2004–12.
37 Leland PA, Raines RT. Cancer chemotherapy – ribonucleases to the rescue. *J Chem Biol* 2001; **8**: 405–13.
38 Leland PA, Staniszewski KE, Kim BM, Raines RT. Endowing human pancreatic ribonuclease with toxicity for cancer cells. *J Biol Chem* 2001; **276**: 43095–102.
39 Rybak SM, Newton DL. Natural and engineered cytotoxic ribonucleases: therapeutic potential. *Exp Cell Res* 1999; **253**: 325–35.
40 Futami J, Maeda T, Kitazoe M *et al.* Preparation of potent cytotoxic ribonucleases by cationization: enhanced cellular uptake and decreased interaction with ribonuclease inhibitor by chemical modification of carboxyl groups. *Biochemistry* 2001; **40**: 7518–24.
41 Folkman J. What is the evidence that tumors are angiogenesis dependent? *J Natl Cancer Inst* 1990; **82**: 4–6.
42 D'Amore PA, Shima DT. Tumor angiogenesis: a physiological process or genetically determined? *Cancer Metastasis Rev* 1996; **15**: 205–12.
43 Hori A, Sasada R, Matsutani E *et al.* Suppression of solid tumor growth by immunoneutralizing monoclonal antibody against human basic fibroblast growth factor. *Cancer Res* 1991; **51**: 6180–4.
44 Noguchi Y, Wu J, Duncan R *et al.* Early phase tumor accumulation of macromolecules: a great difference in clearance rate between tumor and normal tissues. *Jpn J Cancer Res* 1998; **89**: 307–14.
45 Dreher MR, Liu W, Michelich CR, Dewhirst MW, Yuan F, Chilkoti A. Tumor vascular permeability, accumulation, and penetration of macromolecular drug carriers. *J Natl Cancer Inst* 2006; **98**: 335–44.

doi: 10.1111/j.1349-7006.2006.00336.x

Biochemistry **2006,** *45,* 6124−6132

Denatured and Reversibly Cationized p53 Readily Enters Cells and Simultaneously Folds to the Functional Protein in the Cells†

Hitoshi Murata,‡ Masakiyo Sakaguchi,§ Junichiro Futami,‡,||,⊥ Midori Kitazoe,‡ Takashi Maeda,‡ Hideki Doura,‡ Megumi Kosaka,‡ Hiroko Tada,‡ Masaharu Seno,‡,# Nam-ho Huh,§ and Hidenori Yamada*,‡,⊥

Department of Bioscience and Biotechnology, Faculty of Engineering, Graduate School of Natural Science and Technology, Okayama University, Okayama 700-8530, Japan, Department of Cell Biology, Graduate School of Medicine and Dentistry, Okayama University, Okayama 700-8558, Japan, Nippon Shokubai Co., Ltd., 5-8 Nishi Otabi-cho, Suita, Osaka 564-8512, Japan, Engineering Innovation Center, Okayama University, Okayama 700-853, Japan, and Research Center for Biomedical Engineering, Okayama University, Okayama 700-8530, Japan

Received December 27, 2005; Revised Manuscript Received March 14, 2006

ABSTRACT: Cationization is a powerful strategy for internalizing a protein into living cells. On the other hand, a reversibly cationized denatured protein through disulfide bonds is not only soluble in water but also able to fold to the native conformation in vitro. When these advantages in cationization were combined, we developed a novel method to deliver a denatured protein into cells and simultaneously let it fold to express its function within cells. This "in-cell folding" method enhances the utility of recombinant proteins expressed in *Escherichia coli* as inclusion bodies; that is, the recombinant proteins in inclusion bodies are solubilized by reversible cationization through cysteine residues by disulfide bonds with aminopropyl methanethiosulfonate or pyridyldithiopropionylpolyethylenimine and then incubated with cells without an in vitro folding procedure. As a model protein, we investigated human tumor-suppressor p53. Treatment of p53-null Saos-2 cells with reversibly cationized p53 revealed that all events examined as indications of the activation of p53 in cells, such as reduction of disulfide bonds followed by tetramer formation, localization into the nucleus, induction of p53 target genes, and induction of apoptosis of cells, occurred. These results suggest that reversible cationization of a denatured protein through cysteine residues is an alternative method for delivery of a functional protein into cells. This method would be very useful when a native folded protein is not readily available.

It was proposed more than a decade ago that a cationization method can be used for delivery of a protein into cells by adsorption-mediated endocytosis (*1*). To deliver a protein into living cells and let it function within cells, we have developed a method in which a protein is modified with a cationic amine such as ethylenediamine or polyethylenimine (PEI)[1] (*2*−*5*). The method exploits the electrostatic interaction of a cationized protein with the negatively charged cell membrane. From PEI cationization, a protein with a native structure and function was efficiently delivered into cells. However, purification of a large amount of a protein and preservation of its activity during the cationization procedures are sometimes difficult.

The technique of recombinant-protein expression in *Escherichia coli* is widely used to obtain a large amount of protein. However, overexpression of recombinant proteins in *E. coli* often results in the accumulation of insoluble inclusion bodies. Because most denatured proteins are hardly soluble in water, it is difficult to purify them by conventional chromatographic procedures. We have reported that introduction of an efficient positive charge by S-alkylation can solubilize reduced and denatured proteins in water (*6*). We have also developed a method for solubilization of a reduced and denatured protein by reversible modification of cysteine residues with a cationic charge through disulfide bonds. The latter solubilized denatured protein could be not only purified but also further folded to the native conformation in vitro (*7*−*11*).

† This work was performed as a part of a research and development project of the Industrial Science and Technology Program supported by the New Energy and Industrial Technology Development Organization (NEDO). This work was partly supported by grants-in-aid from the Ministry of Education, Science, and Culture of Japan (17360399 to H.Y.).

* To whom correspondence should be addressed. Telephone: +81-86-251-8215. Fax: +81-86-251-8265. E-mail: yamadah@cc.okayama-u.ac.jp.

‡ Graduate School of Natural Science and Technology, Okayama University.

§ Graduate School of Medicine and Dentistry, Okayama University.

|| Nippon Shokubai Co., Ltd.

⊥ Engineering Innovation Center, Okayama University.

Research Center for Biomedical Engineering, Okayama University.

[1] Abbreviations: BSA, bovine serum albumin; DMEM, Dulbecco's modified Eagle's medium; DTT, dithiothreitol; EDTA, ethylenediaminetetraacetic acid; EGTA, ethyleneglycol bis(2-aminoethylether)-tetraacetic acid; FBS, fetal bovine serum; GAPDH, glyceraldehyde-3-phosphate dehydrogenase; 4NQO, 4-nitroquinoline 1-oxide; PBS, phosphate-buffered saline; PEI, polyethylenimine; PEI600, PEI with an average molecular mass of 600; p21/waf1, wild-type p53-activated fragment 1; PTD, protein transduction domain; SPDP, *N*-succinimidyl 3-(2-pyridyldithio)propionate; SDS−PAGE, sodium dodecyl sulfate−polyacrylamide gel electrophoresis; SV40, simian virus 40; SVLT, SV40 large-T antigen; Tris, tris(hydroxymethyl)aminomethane; TRITC, tetramethylrhodamine B isothiocyanate.

10.1021/bi052642a CCC: $33.50
Published on Web 04/25/2006

Cells should have inherent folding machinery for denatured proteins. Thus, using reversible cationization, we developed an "in-cell folding" method for a denatured protein, a method to deliver an unfolded protein into cells and let it fold within cells. Using this method, the human tumor-suppressor p53 expressed in *E. coli* as inclusion bodies was successfully delivered into and folded to the active form within p53-null Saos-2 cells.

MATERIALS AND METHODS

Materials. PEI with an average molecular mass of 600 (PEI600) was purchased from Wako Chemical (Osaka, Japan). *N*-Succinimidyl 3-(2-pyridyldithio)propionate (SPDP) was purchased from Pierce (Rockford, IL). An antibody that recognizes the native conformation of wild-type human p53 (anti-native p53 antibody Ab-5) was purchased from Calbiochem (La Jolla, CA). For Western blot analysis, mouse anti-human p53 antibody (anti-p53 antibody Bp53-12, a product of Santa Cruz Biotechnology, Inc.), mouse anti-human tubulin antibody (anti-tubulin antibody), and mouse anti-human β-actin antibody (anti-β-actin antibody) were purchased from Sigma (St. Louis, MO). Mouse anti-p21/wild-type p53-activated fragment 1 antibody clone 6B6 (anti-p21/waf1 antibody 6B6) was purchased from Becton Dickinson (San Jose, CA). For immunofluorescence staining of cells, mouse anti-p21/wild-type p53-activated fragment 1 antibody clone 187 (anti-p21/waf1 antibody 187) was purchased from Santa Cruz Biotechnology, Inc. (Santa Cruz, CA).

Human osteogenic sarcoma-derived Saos-2 cells were obtained from American Type Culture Collection ATCC (Rockville, MD). Normal human fibroblast OUMS-24 cells were those as described elsewhere (*12*). A plasmid encoding human wild-type full-length p53 (pCB6 + p53Pro) was provided by Dr. Karen Vousden.

Synthesis of 3-Aminopropyl Methanethiosulfonate Hydrobromide (APS-Sulfonate) and Pyridyldithiopropionylpolyethylenimine (PEI600-SPDP). APS-sulfonate was synthesized according to the method for the synthesis of 3-(trimethylammonio)propyl methanethiosulfonate bromide [CH_3SO_2-$SCH_2CH_2CH_2N^+(CH_3)_3 \cdot Br^-$] (TAPS-sulfonate) (*7*), except for the use of 3-bromopropylamine hydrobromide instead of (3-bromopropyl)trimethylammonium bromide. APS-sulfonate was obtained as white crystals from ethanol ether in about 80% yield and melted at 121−124 °C. PEI600-SPDP solution was prepared by just mixing a PEI600 solution (200 mg/mL, 0.33 M, pH 8 adjusted by HCl) with SPDP dissolved in ethanol (0.02 M, at a molar ratio of 5:1 PEI600/SPDP). The solution was incubated at room temperature for 20 min and then stored at 4 °C until use.

Protein Expression and Isolation of Inclusion Bodies. The expression plasmid for p53, pBO429, was constructed by the following digestion and ligation steps. The coding region for human wild-type full-length p53 was excised from pCB6 + p53Pro, at the *Nco*I (by partial digestion) and *Bam*HI sites, and the fragment obtained was inserted between the *Nco*I and *Bam*HI sites of an overexpression vector, pET14b (Novagen, WI). Recombinant p53 was expressed in *E. coli* BL21(DE3) (Novagen) harboring pBO429. For overexpression of p53, the cells were cultured at 37 °C in terrific broth containing 200 μg/mL of ampicillin until A_{600} reached 0.8 and were then treated with 0.5 mM isopropyl 1-thio-β-D-galactopyranoside and cultured for another 3 h. The cells were then pelleted and lysed by repeating a freeze/thaw/sonication cycle twice. The isolation of inclusion bodies was performed according to the published procedure (*13*, *14*).

Reversible Cationization of Protein. The recombinant p53 in the inclusion bodies was dissolved in 0.1 M tris(hydroxymethyl)aminomethane (Tris)-HCl buffer at pH 8.6 containing 6 M guanidine-HCl and reduced with 3 mM dithiothreitol (DTT) at 37 °C for 1 h under N_2 atmosphere. Sulfhydryl (SH) groups of p53 were then modified with APS-sulfonate or PEI600-SPDP to give AP-SS-p53 or PEI600-SS-p53, respectively, which were denatured and reversibly cationized p53 proteins containing cationic groups through disulfide (SS) bonds (Figure 1A). Namely, the reaction was initiated by adding 9 mM APS-sulfonate or PEI600-SPDP to the above denatured and reduced p53 solution, and the solution was incubated at 37 °C for 1 h. In the reaction with a relatively large size of PEI600-SPDP, the modification of cysteine residues in p53 was incomplete, probably because of steric hindrance (see below), and the remaining SH groups catalyzed protein polymerization by SH−SS interchange during the following purification procedures. Thus, after cationization with PEI600-SPDP, possible remaining free SH groups were completely protected by the reaction with a smaller size of APS-sulfonate at 3 mM for another 20 min. After cationization, the mixture was dispersed into 10% acetic acid at pH 3 with vigorous stirring. After removal of insoluble materials by centrifugation, reversibly cationized p53 proteins were concentrated by lyophilization, dissolved in a small amount of Milli-Q water, extensively dialyzed against 0.5% acetic acid at pH 4 to remove excess reagents, and purified by a reversed-phase HPLC column (YMC-Pack ODS-A, YMC, Kyoto, Japan) under a linear-gradient elution of acetonitrile from 30 to 40% in the presence of 0.1% HCl. After exchange of the solvent to phosphate-buffered saline (PBS, pH 7.4) by dialysis or a PD-10 column (Amersham Bioscience, Buckinghamshire, U.K.), the purified reversibly cationized p53 proteins, AP-SS-p53 and PEI600-SS-p53, were used for biological experiments. The number of cysteine residues modified with PEI600 in PEI600-SS-p53 was determined by MALDI−TOF mass spectrometry with a Perspective Voyager-DE PRO mass spectrometer.

As a control protein, bovine serum albumin (BSA) was also reversibly cationized with PEI600-SPDP to give PEI600-SS-BSA, which is a reduced and denatured BSA derivative reversibly cationized with PEI through SS bonds. That is, BSA was reduced with DTT in 0.525 M Tris-HCl (pH 8.6) containing 8 M urea (*6*) and reversibly cationized with PEI600-SPDP for 30 min. In this case, possible remaining SH groups were irreversibly modified by incubation with iodoacetamide for 15 min, and the exchange of the solvent to PBS was carried out by a PD10 column.

Folding Ability of Reversibly Cationized p53 Protein In Vitro. To test the spontaneous folding ability of denatured and reversibly cationized p53 proteins under cytosolic redox conditions, rapid dilution of PEI600-SS-p53 into PBS (pH 7.4) containing 2.5 mM reduced glutathione and 0.05 mM oxidized glutathione at a final protein concentration of 20 μg/mL at 20 °C was carried out. Aliquots were withdrawn at appropriate intervals and subjected to sodium dodecyl sulfate−polyacrylamide gel electrophoresis (SDS−PAGE)

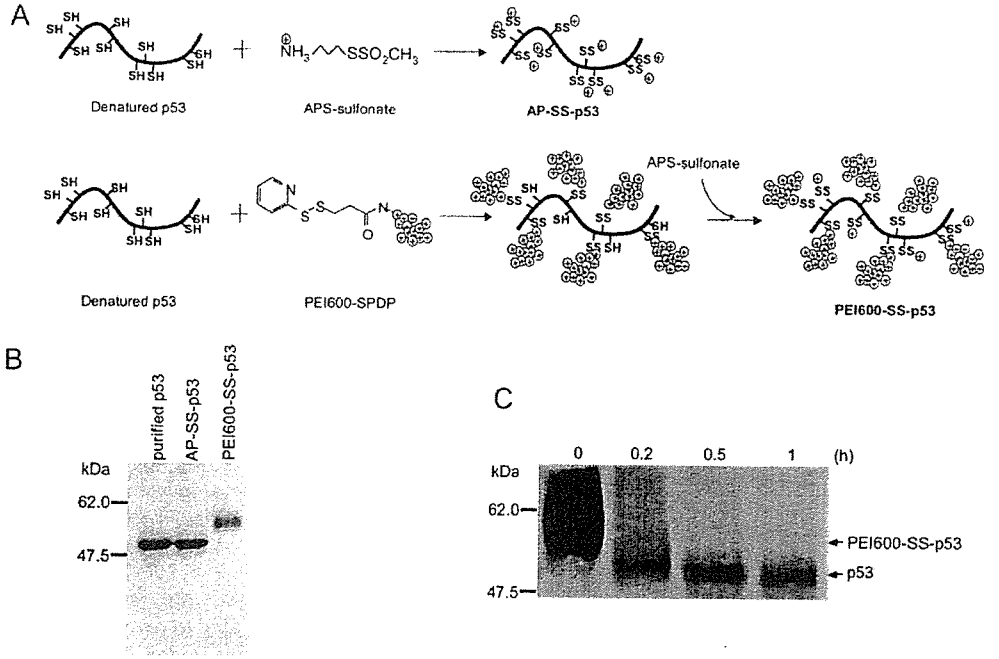

FIGURE 1: Preparation and characterization of denatured and reversibly cationized p53 proteins. (A) Reduced and denatured p53 obtained from inclusion bodies was reversibly cationized in mixed disulfide bonds with APS-sulfonate to give AP-SS-p53 or with PEI600-SPDP followed by APS-sulfonate to give PEI600-SS-p53. (B) SDS−PAGE analysis of purified recombinant p53 and its derivatives (AP-SS-p53 and PEI600-SS-p53) on 10% polyacrylamide gel under nonreducing conditions. The gel was stained with Coomassie Briliant Blue R250. (C) Time-dependent reduction of PEI600-SS-p53 in vitro under cytosolic redox conditions. PEI600-SS-p53 was incubated in a mixture of 2.5 mM reduced glutathione and 0.05 mM oxidized glutathione at pH 7.4 and 20 °C for indicated periods and subjected to SDS−PAGE followed by Western blot analysis using mouse anti-p53 antibody Bp53-12 as a primary antibody and horseradish peroxidase-conjugated goat anti-mouse IgG antibody as a secondary antibody. Details are given in the text.

under nonreducing conditions. The gel was blotted onto a nitrocelulose membrane for Western blot analysis using mouse anti-p53 antibody Bp53-12 as a primary antibody, horseradish peroxidase-conjugated goat anti-mouse IgG antibody (Cell Signaling) as a secondary antibody, and an enhanced chemiluminescence kit (Amersham Biosciences).

Cell Culture and Protein Transduction. p53-null human osteosarcoma Saos-2 and Saos-2/simian virus 40 large-T antigen (SVLT) cells and normal human fibroblast OUMS-24 cells (*12*) were cultured in Dulbecco's modified Eagle's medium (DMEM, Nissui Pharmaceutical, Tokyo, Japan) containing 10% fetal bovine serum (FBS, Sigma). For establishment of Saos-2/SVLT cells, a plasmid encoding SVLT and a G418 resistance marker was introduced into Saos-2 cells using LipofectAMIN 2000 (Invitrogen, CA), and a stably transfected clone was isolated. All cells were cultured in a humidified 5% CO_2 incubator at 37 °C. For protein transduction experiments, about 80% confluent cells were washed once with serum-free medium and then a cationized protein was added under serum-free conditions. After incubation for 1 h at 37 °C, FBS was added at a final concentration of 10% and cells were further incubated for appropriate periods.

Immunoprecipitation and Western Blot Analysis. Cell lysates were prepared using lysis buffer containing 40 mM Tris-HCl at pH 7.4, 1% TritonX-100, 150 mM NaCl, 1 mM ethylenediaminetetraacetic acid (EDTA), 1 mM ethyleneglycol bis(2-aminoethylether)tetraacetic acid (EGTA), 1 mM DTT, and 10% glycerol and were clarified by centrifugation. For immunoprecipitation, cell lysates were precleared with protein G-Sepharose beads (Amersham Biosciences) and then incubated with anti-native p53 antibody Ab-5 for 1 h at 4 °C on a rotating rocker, followed by an additional incubation with protein G-Sepharose beads for 1 h. The immune complexes as well as cell extracts were subjected to SDS−PAGE and transferred onto nitrocellulose membranes. For Western blot analysis, after blocking with 10% skim milk powder and 6% glycine dissolved in PBS, membranes were incubated with anti-p53 antibody Bp53-12, anti-p21/waf1 antibody 6B6, anti-β-actin antibody, or anti-tubulin antibody as primary antibodies. Each specific antibody binding was detected with horseradish peroxidase-conjugated goat anti-mouse IgG antibody and an enhanced chemiluminescence kit as described above.

Cross-Linking Analysis. For analysis of the quaternary structure of exogenously added p53, cells were treated with 1 mM glutaraldehyde for 10 min at 25 °C to preserve the molecular interaction by cross-linking. The reaction was terminated by the addition of 0.1 M glycine. Cell lysates prepared were analyzed by Western blot analysis using anti-p53 antibody Bp53-12. The normal human fibroblast OUMS-24 cells were incubated under confluent or serum-starved conditions for 24 h or the cells were treated with 10 μM 4-nitroquinoline 1-oxide (4NQO) for 6 h. These cells were used as positive controls. Saos-2 and OUMS-24 cells incubated without additives or Saos-2 cells incubated with PEI600-SS-BSA were used as negative controls.

Immunofluorescence Staining. Cells were fixed with 4% paraformaldehyde for 1 h at room temperature and then permeabilized with 70% ethanol at −20 °C. Immunofluorescence staining for exogenously added p53 or endogenously expressed p21/waf1 was performed by treatment of cells with

mouse anti-p53 antibody Bp53-12 or mouse anti-p21/waf1 antibody 187, respectively, followed by treatment with tetramethylrhodamine B isothiocyanate (TRITC)-conjugated goat anti-mouse IgG antibody (Sigma). Nuclei were stained with Hoechst 33258 (Dojin Laboratories, Kumamoto, Japan). The cells were observed under a fluorescent microscope (IX71-22FL/PH, Olympus).

Northern Blotting. Total RNA was isolated using the guanidium thiocyanate method (*15*). Total RNA was separated by electrophoresis (15 μg/lane) in a 1% formaldehyde-agarose gel and then transferred to a nylon membrane (Nytran-Plus, Schleicher and Schuell, Keene, NH). The blots were probed with gel-purified [γ-^{32}P]dCTP-labeled cDNAs for p21/waf1 mRNA. Membranes were subsequently stripped and reprobed for glyceraldehyde-3-phosphate dehydrogenase (GAPDH) for normalization.

Electrophoresis Mobility Shift Assay. An electrophoresis mobility shift assay was performed as described by Nakano et al. (*16*) using crude nuclear extracts from cells treated with 100 nM PEI600-SS-p53, 100 nM PEI600-SS-BSA, or 10 μM 4NQO for 6 h. We used a double-strand oligonucleotide for the p53-binding element as a probe (Santa Cruz Biotechnology, Inc.). The consensus sequence is 5′-TACA-GAACATGTCTAAGCATGCTGGGG-3′. The [γ-^{32}P]dATP-labeled probe was mixed with crude nuclear extracts of Saos-2 or OUMS-24 cells, incubated for 1 h at 4 °C, and electrophoresed in a 5% polyacrylamide gel under nondenaturing conditions.

Apoptosis Analysis with DNA-Ladder Formation. The cells at various stages were harvested and incubated with lysis buffer containing 10 mM Tris-HCl at pH 7.4, 5 mM EDTA, and 1% TritonX-100 for 20 min on ice. The supernatant containing DNA fragments was incubated with 10 μg/mL RNase A for 1 h at 37 °C. After further incubation with 20 μg/mL proteinase K for 1 h at 37 °C, samples were washed with phenol−chloroform and DNA was precipitated with ethanol. Recovered DNA was electrophoresed on 2% agarose gel and stained with ethidium bromide.

RESULTS

Preparation of Denatured and Reversibly Cationized p53. As summarized in Figure 1A, reversibly cationized p53 proteins were prepared from inclusion bodies dissolved in 6 M guanidine-HCl by alkylsulfidation of sulfhydryl groups with APS-sulfonate and PEI600-SPDP, respectively. Because the modification of p53 with PEI600-SPDP was found to be incomplete (approximately 6 of 10 cysteine residues) probably because of steric hindrance, the remaining 4 free sulfhydryl groups were completely protected with a smaller size of APS-sulfonate. Formation of mixed disulfides with positively charged side-chain groups, especially with PEI, in the polypeptide chain resulted in slower migration on SDS−PAGE under nonreducing conditions (Figure 1B). Both cationized p53 proteins (AP-SS-p53 and PEI600-SS-p53) showed good solubility in water, especially at acidic pH values, because of an increase in the net positive charge by protonation of carboxyl groups. We have confirmed that reversibly cationized p53 proteins remained soluble in 0.5% acetic acid for more than 6 months at 4 °C.

Upon rapid dilution in vitro, reduced p53 purified from inclusion bodies has been reported to have the ability to fold into the biologically active conformation (*17*). Thus, for reversibly cationized p53 proteins to fold in vivo, it is important that they are able to revert to unprotected reduced p53 under cytosol-mimic redox conditions (50:1 reduced glutathione/oxidized glutathione) (*18*). As mentioned above (Figure 1B), PEI600-SS-p53 migrates slower than p53 on SDS−PAGE, and hence, reduction of PEI600-SS-p53 can be monitored. Upon dilution of PEI600-SS-p53 into the redox buffer, PBS (pH 7.4) containing 2.5 mM reduced glutathione and 0.05 mM oxidized glutathione, at a final protein concentration of 20 μg/mL at 20 °C, rapid removal of protecting groups by reduction was observed, and this reduction seemed to be completed in about 1 h to give unprotected p53 (Figure 1C). No precipitation was observed during the process. These results suggest that the reversibly cationized p53 proteins can be reduced to free p53 if they internalized into the cytosol and therefore might fold into the native p53.

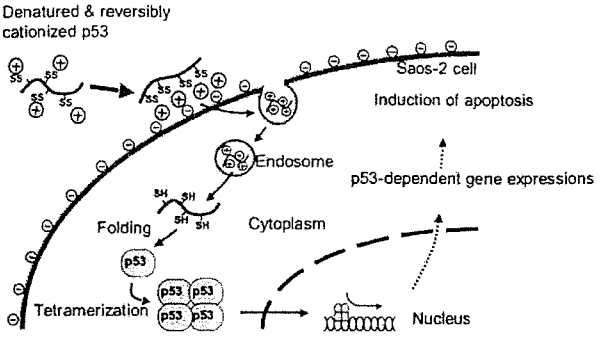

FIGURE 2: Schematic diagram of the "in-cell folding" method for the p53 tumor-suppressor protein. The essential steps for externally added denatured and reversibly cationized p53 to express the native protein functions in Saos-2 cells (electrostatic cell-surface adsorption and/or endosome accumulation, reduction of disulfide bonds because of the release to cytosol, folding and tetramer formation, localization into the nucleus, induction of p53 target genes, and induction of apoptosis of cells) are depicted.

Intracellular Protein Delivery of Reversibly Cationized p53. To investigate whether reversibly cationized p53 proteins could internalize into cells and simultaneously fold into the biologically active structure, we tested essential steps of known p53-dependent cellular responses, as depicted in Figure 2. We employed Saos-2 cells for this assay, because of the lack of endogenous p53 (*19*).

As visualized by immunofluorescence staining, Saos-2 cells showed marked cellular uptake of p53 when exposed to either AP-SS-p53 or PEI600-SS-p53 for 6 h (Figure 3A). Although these fluorescence patterns observed using a fluorescence microscope did not enable p53 internalized in cytoplasmic compartments to be distinguished from the cell-surface associated one, observation of PEI600-SS-p53-treated cells using a confocal laser-scanning microscope indicated that fluorescence was mostly present inside cells (data not shown). The more cationic PEI600-SS-p53 seemed more effective in cellular uptake than did AP-SS-p53 (Figure 3A).

We have previously demonstrated that PEI-cationized proteins enter living cells and have shown that the major mechanism of the protein internalization is endocytotic uptake and subsequent release into the cytosol from endosomes (*4*, *5*). If the reversibly cationized p53 proteins internalize via an endocytotic pathway, the entrapped proteins

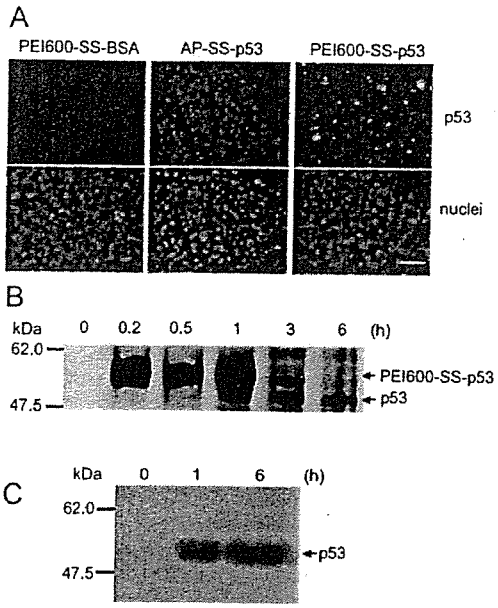

FIGURE 3: Cellular uptake, reduction, and folding of exogenously added reversibly cationized p53 proteins to Saos-2 cells. (A) Saos-2 cells were incubated with 100 nM PEI600-SS-BSA, AP-SS-p53, or PEI600-SS-p53 for 6 h, fixed, immunostained with mouse anti-p53 antibody Bp53-12 and TRITC-conjugated anti-mouse IgG antibody, and observed under a fluorescent microscope (upper panels). Nuclei stained with Hoechst 33258 are also indicated (lower panels). The scale bar is equivalent to 50 μm. (B) Time course of the reduction of PEI600-SS-p53 in cells. Saos-2 cells were incubated with 100 nM PEI600-SS-p53 for indicated periods, and the reduction of PEI600-SS-p53 was analyzed by Western blot analysis with anti-p53 antibody Bp53-12 after SDS−PAGE of cell lysates under nonreducing conditions. (C) Detection of intracellularly folded p53. After incubation of Saos-2 cells with 100 nM PEI600-SS-p53 for indicated periods, folded p53 was collected from cell lysates by immunoprecipitation using anti-native p53 antibody Ab-5 and protein G-Sepharose beads. The precipitates were then electrophoresed by SDS−PAGE under reducing conditions, blotted to nitrocellulose membranes, and analyzed by Western blot analysis with anti-p53 antibody Bp53-12.

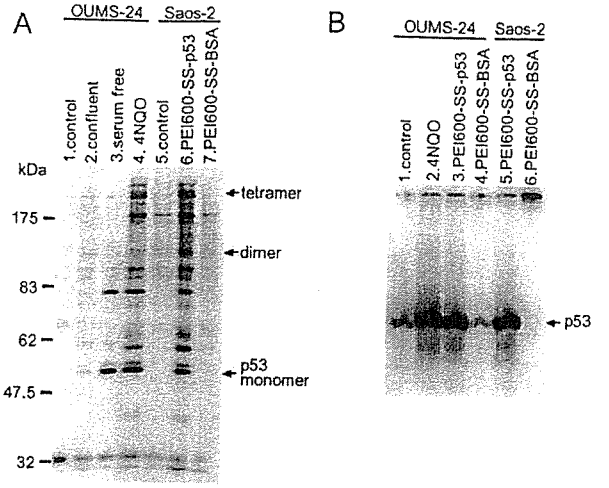

FIGURE 4: Analysis of the quaternary structure and DNA binding of folded p53. (A) Oligomeric states of internalized p53 in cells determined by cross-linking analysis. Normal human fibroblast OUMS-24 cells were incubated under nonconfluent conditions for 6 h (negative control, lane 1), under confluent conditions for 24 h (positive control, lane 2), or under serum-starved conditions for 24 h (positive control, lane 3) or were treated with 10 μM 4NQO for 6 h (positive control, lane 4). p53-null Saos-2 cells were incubated without additives (negative control, lane 5), with 100 nM PEI600-SS-p53 (lane 6), or with PEI600-SS-BSA (negative control, lane 7) for 6 h. The cells were treated with 1 mM glutaraldehyde and then lysed, and cell lysates were analyzed by Western blot analysis using anti-p53 antibody Bp53-12. Arrows indicate positions of the tetramer, dimer, and monomer of p53, which were separately determined by using p53 cross-linked with glutaraldehyde in vitro (data not shown). (B) Electrophoresis mobility shift assay of the p53-binding element with internalized p53 in cells. Crude nuclear extracts from OUMS-24 cells incubated without additives (lane 1), with 10 μM 4NQO (lane 2), with 100 nM PEI600-SS-p53 (lane 3), or with 100 nM PEI600-SS-BSA (lane 4) for 6 h or those from Saos-2 cells incubated with 100 nM PEI600-SS-p53 (lane 5) or 100 nM PEI600-SS-BSA (lane 6) for 6 h were incubated with [γ-^{32}P]dATP-labeled double-strand oligonucleotide for the p53-binding element for 1 h at 4 °C and then electrophoresed in a 5% polyacrylamide gel under nondenaturing conditions. The [γ-^{32}P]dATP-labeled p53-binding element in the gel was detected autoradiographically. Arrow indicates the position of p53.

in the endosome would remain inactive because disulfide bonds are scarcely reduced under endosomal oxidative conditions, but they might fold to the active conformation in the cytosol because disulfide bonds are readily reduced under cytosolic reductive conditions (Figure 1C). Thus, reduction of mixed disulfide bonds in reversibly cationized p53 proteins should be good proof of their cytosolic release. Western blot analysis of SDS−PAGE for PEI600-SS-p53-treated Saos-2 cells indicated that the band corresponding to PEI600-SS-p53 because of cell-surface adsorption and/or endosome accumulation was the main band for the first 1 h of incubation but that the band corresponding to reduced p53 because of cytosolic release became the main band after 3 and 6 h of incubation (Figure 3B).

To confirm time-dependent folding of reversibly cationized p53 proteins in Saos-2 cells, folded p53 in the cell lysate was immunoprecipitated with a specific antibody recognizing the native conformation (anti-native p53 antibody Ab-5) after incubation of cells with 100 nM PEI600-SS-p53 for 1 and 6 h, and the precipitates were analyzed by Western blotting analysis using anti-p53 antibody Bp53-12 (Figure 3C). Time-dependent formation of p53 assuming native conformation was clearly observed, being well-correlated with the reduction of PEI600-SS-p53 in the cytosol (Figure 3B). All of these observations suggest that exogenously added reversibly cationized p53 proteins are rapidly adsorbed on the cell surface by the electrostatic interaction, endocytozed by cells up to 1 h at 37 °C, and more slowly released into the cytosol, where reduction of mixed disulfide bonds followed by folding to the biologically active form takes place.

Quaternary Structure and Specific DNA Binding of Intracellularly Folded p53. The transcriptional activity of p53 has been reported to be associated with a tetrameric form that binds DNA in a sequence-specific fashion to activate the transcription of target genes (*20*−*23*). To confirm the formation of tetrameric p53 when delivered into cells as described above, we performed cross-linking experiments with glutaraldehyde as a cross-linking agent to fix the protein quaternary structure. As shown in Figure 4A, the electrophoretic pattern obtained from PEI600-SS-p53-treated Saos-2 cells indicated the presence of a covalently cross-linked p53 dimer and tetramer including possibly their degraded products (lane 6). No such pattern was obtained from Saos-2 cells treated without cationized protein (one negative control, lane

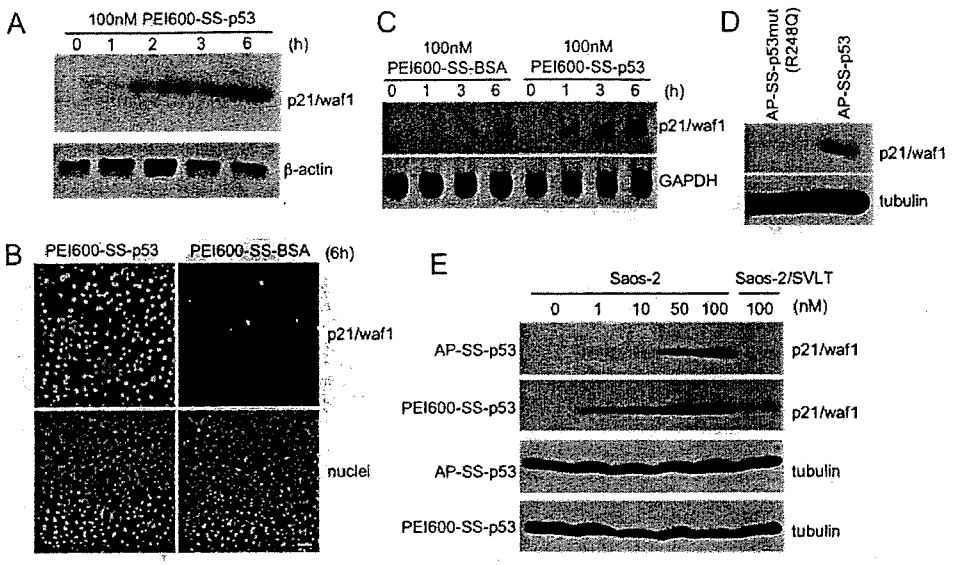

FIGURE 5: Induction of the p53-dependent gene expression of p21/waf1. Saos-2 cells were incubated with 100 nM PEI600-SS-p53 or PEI600-SS-BSA for indicated periods, and induction of p21/waf1 was examined at the protein level (A and B) or mRNA level (C). (A) Western blot analysis of the time-dependent expression of the p21/waf1 protein in Saos-2 cells by treatment with 100 nM PEI600-SS-p53. Expression of p21/waf1 (upper panel) was examined by SDS−PAGE of cell lysates and Western blot analysis with anti-p21/waf1 antibody 6B6. The expression level of β-actin (lower panel) was examined by reprobing using anti-β-actin antibody for normalization. (B) Saos-2 cells were incubated with 100 nM PEI600-SS-p53 (left panels) or PEI600-SS-BSA (right panels) for 6 h, fixed, immunostained with mouse anti-p21/waf1 antibody 187 and TRITC-conjugated anti-mouse IgG antibody, and then observed under a fluorescent microscope (upper panels). Nuclei stained with Hoechst 33258 are also indicated (lower panels). The bar indicates 80 μm. (C) Northern blot analysis for examination of the time-dependent expression of p21/waf1 mRNA in PEI600-SS-p53-treated Saos-2 cells. Total RNAs isolated from cells treated with 100 nM PEI600-SS-BSA or PEI600-SS-p53 for indicated periods were separated by electrophoresis and transferred to nylon membranes. The blots were probed with [γ-^{32}P]dCTP-labeled cDNAs for p21/waf1 (upper panel). Membranes were subsequently stripped and reprobed for GAPDH for normalization (lower panel). (D) Transactivation activity of the p53-dependent p21/waf1 protein expression. Saos-2 cells were incubated with 100 nM AP-SS-p53 (upper panel, right) or transactivation-deficient AP-SS-p53 mutant [AP-SS-p53mut (R248Q)] (upper panel, left) for 6 h and analyzed by Western blot analysis using anti-p21/waf1 antibody 6B6. Tubulin was employed for normalization (lower panel). (E) Dose dependence of p21/waf1 protein expression in reversibly cationized p53-treated Saos-2 cells and lack of p53 function in reversibly cationized p53-treated Saos-2/SVLT cells. Saos-2 cells and Saos-2/SVLT cells that express SVLT suppressing the p53 function were incubated with AP-SS-p53 or PEI600-SS-p53 at indicated concentrations for 6 h. After SDS−PAGE of cell lysates, expression levels of p21/waf1 were analyzed by Western blot analysis using anti-p21/waf1 antibody 6B6 (top panel for AP-SS-p53 and second-to-top panel for PEI600-SS-p53). Tubulin was employed for normalization (bottom and second-to-bottom panels).

5) or from Saos-2 cells treated with cationized BSA (another negative control, lane 7). However, the same pattern was obtained from normal OUMS-24 cells that the endogenous p53 level was upregulated by 4NQO (a positive control, lane 4) (*12*, *24*). These results suggest that externally added reversibly cationized p53 folds intracellularly to a tetrameric form. Interestingly, the pattern obtained from confluent OUMS-24 cells (one of the positive controls, lane 2) seemed similar to the pattern from PEI600-SS-p53-treated cells, although the level of tetrameric p53 was very low, while the pattern obtained from serum-starved OUMS-24 cells (another positive control, lane 3) seemed different from those of other positive controls in the distribution of p53 oligomers and degraded products. The growth-arrested state in serum-starved cells might not be the same as that in confluent cells.

Next, we investigated the specific binding ability of intracellularly folded p53 to a DNA fragment of the p53-binding element. As shown in Figure 4B, the nuclear extract obtained from Saos-2 cells treated with PEI600-SS-p53 for 6 h contained p53 showing specific binding activity against the labeled DNA fragment (lane 5). Similar results were also obtained by using nuclear extracts from 4NQO-treated OUMS-24 cells (positive control, lane 2) and from PEI600-SS-p53-treated OUMS-24 cells (lane 3). The nuclear extract from OUMS-24 cells incubated without cationized protein (lane 1) or with cationized BSA (lane 4) showed a background level of active p53 in the cells. The nuclear extract from cationized BSA-treated Saos-2 cells did not give the band corresponding to p53 (lane 6). These results imply that the intracellularly folded p53 was translocated to the nucleolus as a biologically active tetramer when cells were incubated with PEI600-SS-p53 for 6 h.

Induction of Intracellularly Delivered p53-Dependent Gene Expression. If exogenously added reversibly cationized p53 proteins express their transcriptional activity, one of the known p53 target gene products, p21/waf1, should be upregulated in Saos-2 cells (*20*, *25*). Thus, we examined the effect of treatment of Saos-2 cells with AP-SS-p53 or PEI600-SS-p53 on the expression of p21/waf1 and found that was the case (Figure 5). Time-dependent expression of p21/waf1 was examined by adding 100 nM PEI600-SS-p53 to the culture medium of Saos-2 cells. The cells were harvested several times for Western blot analysis up to 6 h after the addition of PEI600-SS-p53. The protein level of p21/waf1 was gradually elevated by this treatment (Figure 5A). Immunofluorescence experiments revealed that the expression of p21/waf1 was induced in approximately 60% of cells by this treatment for 6 h but not by treatment with PEI600-SS-BSA (Figure 5B). The same was true when the induction of p21/waf1 was monitored by the mRNA level (Figure 5C). Another reversibly cationized p53 protein, AP-SS-p53, also induced p21/waf1 expression in Saos-2 cells,

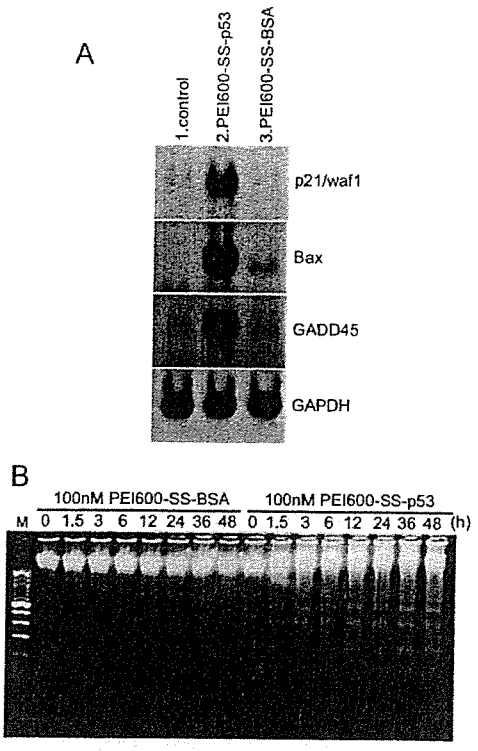

FIGURE 6: Biological effects of introduced p53 on Saos-2 cells. (A) Saos-2 cells were treated without additives (control, lane 1), with 100 nM PEI600-SS-p53 (lane 2), or with PEI600-SS-BSA (lane 3) for 6 h, and transcriptional activation of p53-dependent apoptotic genes (p21/waf1, Bax, and GADD45) was examined by Northern blot analysis. GAPDH was employed for normalization. (B) DNA fragmentation in Saos-2 cells treated with PEI600-SS-p53. After incubation of Saos-2 cells with 100 nM PEI600-SS-p53 or PEI600-SS-BSA for indicated periods, the respective DNAs were extracted and analyzed by electrophoresis on a 2% agarose gel. The gel was stained with ethidium bromide. M indicates molecular markers (the left most lane).

but p21/waf1 expression was not induced when cells were treated with reversibly cationized transactivation-deficient AP-SS-p53 mutant (R248Q) (*26*) (Figure 5D). The latter result is consistent with the failure of AP-SS-p53 or PEI600-SS-p53 to induce p21/waf1 in Saos-2/SVLT cells that express SVLT suppressing p53 function by specific binding (*27*) (Figure 5E). We further compared AP-SS-p53 and PEI600-SS-p53 for dose dependency to the induction of p21/waf1. The more cationic PEI600-SS-p53 showed more efficient activity than did AP-SS-p53 as seen in the treatment with 1 nM for 6 h (Figure 5E). These results demonstrated that exogenous p53 delivered by this method is a highly potent inducer of the target gene expression.

Induction of Apoptosis by Intracellularly Delivered p53-Dependent Gene Expression. Because it has been reported that induction of p53 expression in Saos-2 cells at a low level induces growth arrest but at a high level induces apoptosis (*28*), we analyzed apoptotic gene expression in PEI600-SS-p53-treated Saos-2 cells. Treatment with 100 nM PEI600-SS-p53 but not with 100 nM PEI600-SS-BSA for 6 h caused transcriptional activation of p53-dependent apoptotic genes (p21/waf1, Bax, and GADD45) in Saos-2 cells (Figure 6A). These results were supported by apoptotic DNA-ladder formation in PEI600-SS-p53-treated cells compared with that in PEI600-SS-BSA-treated cells (Figure 6B).

DISCUSSION

The living cell membrane poses a substantial hurdle for exogenous protein to express its function inside cells. To overcome this limitation, a variety of new methodologies to deliver functional proteins into cells are being studied actively. The new methodologies include "protein cationization methods". Methods using 8−35 amino-acid-long peptides called "protein transduction domains" (PTDs) are the most popular (*29*−*35*). PTDs derived from human immunodeficiency virus-transactivator of transcription (HIV-TAT) (*30*, *32*), herpes simplex virus-structural protein VP22 (HSV-VP22) (*31*), and antennapedia (*29*) or synthetic PTDs (*33*−*35*) are characterized by a high content of positively charged arginine and lysine residues, which are potentially important for association with the negatively charged cell-surface membrane by electrostatic interaction followed by internalization into cells by endocytosis (*36*, *37*) or macropinocytosis (*38*). Chemical cationization methods developed by us (*3*−*5*) are also included in this category. A cationic lipid-based carrier system (*39*), virus envelope vector (*40*), and PEI-cationized carrier systems (*5*) have also been proposed. Although these current protein transduction techniques seem promising for laboratory investigations and therapeutic applications, proteins to be delivered into cells require sufficient solubility. Because denatured proteins are hardly soluble in physiological aqueous solutions, detergents or denaturants toxic for living cells are generally used to solubilize them. In the present study, we showed that the denatured form of the reversibly cationized p53 protein was not only soluble in physiological solutions but also active for transduction into living cells to express its functions inside cells because of simultaneous folding. We call this protein transduction method the "in-cell folding" technique. This technique would be of great value especially when proteins to be delivered into cells are not easily available as biologically active conformations in vitro.

Because mutations in p53 are among the most common genetic events in the development of human cancer (*41*), many studies have been carried out to evaluate viral vector-mediated p53 gene delivery for gene therapy (*42*). Approaches for protein transduction therapy using a PTD peptide fused to folded p53 have also been carried out and have been shown to be useful to inhibit the proliferation of cancer cells (*43*−*45*). Although a protein transduction method allows the protein to function in cells transiently, PEI600-SS-p53 could induce p53-target genes only at 1 nM (Figure 5E), suggesting that the method would be effective at limited doses to inhibit cancer cell growth in therapeutic applications.

In this study, we used APS-sulfonate and PEI600-SPDP to cationize denatured p53 (Figure 1A). Both reagents possess moieties with common characteristics, a SH-selective and rapid modifying moiety (methanethiosulfonyl or dithiopyridyl group) and a cationic side-chain moiety (amine or polyamine group). Thus, in the reaction with these reagents, positive charges were introduced into 10 cysteine residues (that is, 10 free SH groups) of p53 through the formation of mixed disulfide bonds to give AP-SS-p53 or PEI600-SS-p53. As shown in Figure 1C, AP-SS-p53 and PEI600-SS-p53 were equivalent to reduced p53 in the SS−SH interchange reaction under cytosolic redox conditions. In other words, denatured

AP-SS-p53, PEI600-SS-p53, and reduced p53 have equivalent folding abilities in the cytosol.

If charged residues at neutral pH are assumed to be only Asp(−1), Glu(−1), Lys(+1), and Arg(+1) for simplicity, the net charge of wild-type p53 is calculated to be −4. APS-sulfonate and PEI600-SPDP can introduce positive charges of +1 and +13.6, respectively, into every cysteine residue. As mentioned above, PEI600-SS-p53 contained approximately six and four cysteine residues modified with PEI600-SPDP and APS-sulfonate, respectively. Thus, net charges of AP-SS-p53 and PEI600-SS-p53 were calculated to be +6 and +81.6, respectively. We previously showed that the net positive charge of proteins correlated well with their efficiency in protein transduction (*2*, *3*, *46*). Consistent with this previous observation, PEI600-SS-p53 seemed to be more effective than AP-SS-p53 (Figures 3A and 5E).

Although various recombinant protein production systems or in vitro translation systems are now available, there is no guarantee that a large amount of biologically active products will be yielded. However, denatured proteins can be easily obtained as inclusion bodies in good yield if an *E. coli* expression system is used. The results presented here demonstrated the possibility of the "in-cell folding" technique; that is, reversibly cationized unfolded proteins could internalize into living cells and simultaneously fold to biologically active conformations. Because many newly synthesized proteins in the cytosol require involvement of complex cellular machinery such as chaperones and processing enzymes as well as input of metabolic energy to reach their native states (*47*) and because such machinery is not easily utilized in vitro, the strategy of "in-cell folding" may be reasonable in some cases. Thus, the "in-cell folding" technique may greatly enhance the utility of a protein expression system, yielding unfolded proteins such as hardly soluble inclusion bodies when protein transduction into living cells is attempted.

REFERENCES

1. Kumagai, A. K., Eisenberg, J. B., and Pardridge, W. M. (1987) Absorptive-mediated endocytosis of cationized albumin and a β-endorphin-cationized albumin chimeric peptide by isolated brain capillaries. Model system of blood-brain barrier transport, *J. Biol. Chem. 262*, 15214−15219.
2. Futami, J., Maeda, T., Kitazoe, M., Nukui, E., Tada, H., Seno, M., Kosaka, M., and Yamada, H. (2001) Preparation of potent cytotoxic ribonucleases by cationization: Enhanced cellular uptake and decreased interaction with ribonuclease inhibitor by chemical modification of carboxyl groups, *Biochemistry 40*, 7518−7524.
3. Futami, J., Nukui, E., Maeda, T., Kosaka, M., Tada, H., Seno, M., and Yamada, H. (2002) Optimum modification for the highest cytotoxicity of cationized ribonuclease, *J. Biochem. 132*, 223−228.
4. Futami, J., Kitazoe, M., Maeda, T., Nukui, E., Sakaguchi, M., Kosaka, J., Miyazaki, M., Kosaka, M., Tada, H., Seno, M., Sasaki, J., Huh, N. H., Namba, M., and Yamada, H. (2005) Intracellular delivery of proteins into mammalian living cells by polyethylenimine-cationization, *J. Bioeng. Biosci. 99*, 95−103.
5. Kitazoe, M., Murata, H., Futami, J., Maeda, T., Sakaguchi, M., Miyazaki, M., Kosaka, M., Tada, H., Seno, M., Huh, N. H., Namba, M., Nishikawa, M., Maeda, Y., and Yamada, H. (2005) Protein transduction assisted by polyethylenimine-cationized carrier proteins, *J. Biochem. 137*, 693−701.
6. Yamada, H., Seno, M., Kobayashi, A., Moriyama, T., Kosaka, M., Ito, Y., and Imoto, T. (1994) An *S*-alkylating reagent with positive charges as an efficient solubilizer of denatured disulfide-containing proteins, *J. Biochem. 116*, 852−857.
7. Inoue, M., Akimaru, J., Nishikawa, T., Seki, N., and Yamada, H. (1998) A new derivatizing agent, trimethylammoniopropyl methanethiosulphonate, is efficient for preparation of recombinant brain-derived neurotrophic factor from inclusion bodies, *Biotechnol. Appl. Biochem. 28*, 207−213.
8. Seno, M., DeSantis, M., Kannan, S., Bianco, C., Tada, H., Kim, N., Kosaka, M., Gullick, W. J., Yamada, H., and Salomon, D. S. (1998) Purification and characterization of a recombinant human cripto-1 protein, *Growth Factors 15*, 215−229.
9. Mallorqui-Fernandez, G., Pous, J., Peracaula, R., Aymami, J., Maeda, T., Tada, H., Yamada, H., Seno, M., de Llorens, R., Gomis-Ruth, F. X., and Coll, M. (2000) Three-dimensional crystal structure of human eosinophil cationic protein (RNase 3) at 1.75 Å resolution, *J. Mol. Biol. 300*, 1297−1307.
10. Miura, K., Doura, H., Aizawa, T., Tada, H., Seno, M., Yamada, H., and Kawano, K. (2002) Solution structure of betacellulin, a new member of EGF-family ligands, *Biochem. Biophys. Res. Commun. 294*, 1040−1046.
11. Newton, D. L., Futami, J., Ruby, D., and Rybak, S. M. (2003) Construction and characterization of RNase-based targeted therapeutics, *Methods Mol. Biol. 207*, 283−304.
12. Bai, L., Mihara, K., Kondo, Y., Honma, M., and Namba, M. (1993) Immortalization of normal human fibroblasts by treatment with 4-nitroquinoline 1-oxide, *Int. J. Cancer 53*, 451−456.
13. Futami, J., Tsushima, Y., Tada, H., Seno, M., and Yamada, H. (2000) Convenient and efficient in vitro folding of disulfide-containing globular protein from crude bacterial inclusion bodies, *J. Biochem. 127*, 435−441.
14. Futami, J., Tada, H., Seno, M., Ishikami, S., and Yamada, H. (2000) Stabilization of human RNase 1 by introduction of a disulfide bond between residues 4 and 118, *J. Biochem. 128*, 245−250.
15. Chirgwin, J. M., Przybyla, A. E., MacDonald, R. J., and Rutter, W. J. (1979) Isolation of biologically active ribonucleic acid from sources enriched in ribonuclease, *Biochemistry 18*, 5294−5299.
16. Nakano, K., Mizuno, T., Sowa, Y., Orita, T., Yoshino, T., Okuyama, Y., Fujita, T., Ohtani-Fujita, N., Matsukawa, Y., Tokino, T., Yamagishi, H., Oka, T., Nomura, H., and Sakai, T. (1997) Butyrate activates the WAF1/Cip1 gene promoter through Sp1 sites in a p53-negative human colon cancer cell line, *J. Biol. Chem. 272*, 22199−22206.
17. Bell, S., Hansen, S., and Buchner, J. (2002) Refolding and structural characterization of the human p53 tumor suppressor protein, *Biophys. Chem. 96*, 243−257.
18. Hwang, C., Sinskey, A. J., and Lodish, H. F. (1992) Oxidized redox state of glutathione in the endoplasmic reticulum, *Science 257*, 1496−1502.
19. Diller, L., Kassel, J., Nelson, C. E., Gryka, M. A., Litwak, G., Gebhardt, M., Bressac, B., Ozturk, M., Baker, S. J., Vogelstein, B., and Friend, S. H. (1990) p53 functions as a cell cycle control protein in osteosarcomas, *Mol. Cell. Biol. 10*, 5772−5781.
20. el-Deiry, W. S., Tokino, T., Velculescu, V. E., Levy, D. B., Parsons, R., Trent, J. M., Lin, D., Mercer, W. E., Kinzler, K. W., and Vogelstein, B. (1993) WAF1, a potential mediator of p53 tumor suppression, *Cell 75*, 817−825.
21. Halazonetis, T. D., and Kandil, A. N. (1993) Conformational shifts propagate from the oligomerization domain of p53 to its tetrameric DNA binding domain and restore DNA binding to select p53 mutants, *EMBO J. 12*, 5057−5064.
22. Friedman, P. N., Chen, X., Bargonetti, J., and Prives, C. (1993) The p53 protein is an unusually shaped tetramer that binds directly to DNA, *Proc. Natl. Acad. Sci. U.S.A. 90*, 3319−3323.
23. Stenger, J. E., Tegtmeyer, P., Mayr, G. A., Reed, M., Wang, Y., Wang, P., Hough, P. V., and Mastrangelo, I. A. (1994) p53 oligomerization and DNA looping are linked with transcriptional activation, *EMBO J. 13*, 6011−6020.
24. Mirzayans, R., Bashir, S., Murray, D., and Paterson, M. C. (1999) Inverse correlation between p53 protein levels and DNA repair efficiency in human fibroblast strains treated with 4-nitroquinoline 1-oxide: Evidence that lesions other than DNA strand breaks trigger the p53 response, *Carcinogenesis 20*, 941−946.
25. Bunz, F., Dutriaux, A., Lengauer, C., Waldman, T., Zhou, S., Brown, J. P., Sedivy, J. M., Kinzler, K. W., and Vogelstein, B. (1998) Requirement for p53 and p21 to sustain G2 arrest after DNA damage, *Science 282*, 1497−1501.
26. Cho, Y., Gorina, S., Jeffrey, P. D., and Pavletich, N. P. (1994) Crystal structure of a p53 tumor suppressor−DNA complex: Understanding tumorigenic mutations, *Science 265*, 346−355.
27. Lane, D. P., and Crawford, L. V. (1979) T antigen is bound to a host protein in SV40-transformed cells, *Nature 278*, 261−263.

28. Chen, X., Ko, L. J., Jayaraman, L., and Prives, C. (1996) p53 levels, functional domains, and DNA damage determine the extent of the apoptotic response of tumor cells, *Genes Dev. 10*, 2438−2451.
29. Derossi, D., Joliot, A. H., Chassaing, G., and Prochiantz, A. (1994) The third helix of the *Antennapedia* homeodomain translocates through biological membranes, *J. Biol. Chem. 269*, 10444−10450.
30. Vives, E., Brodin, P., and Lebleu, B. (1997) A truncated HIV-1 Tat protein basic domain rapidly translocates through the plasma membrane and accumulates in the cell nucleus, *J. Biol. Chem. 272*, 16010−16017.
31. Elliott, G., and O'Hare, P. (1997) Intercellular trafficking and protein delivery by a herpesvirus structural protein, *Cell 88*, 223−233.
32. Schwarze, S. R., Ho, A., Vocero-Akbani, A., and Dowdy, S. F. (1999) In vivo protein transduction: Delivery of a biologically active protein into the mouse, *Science 285*, 1569−1572.
33. Wender, P. A., Mitchell, D. J., Pattabiraman, K., Pelkey, E. T., Steinman, L., and Rothbard, J. B. (2000) The design, synthesis, and evaluation of molecules that enable or enhance cellular uptake: Peptoid molecular transporters, *Proc. Natl. Acad. Sci. U.S.A. 97*, 13003−13008.
34. Futaki, S., Suzuki, T., Ohashi, W., Yagami, T., Tanaka, S., Ueda, K., and Sugiura, Y. (2001) Arginine-rich peptides. An abundant source of membrane-permeable peptides having potential as carriers for intracellular protein delivery, *J. Biol. Chem. 276*, 5836−5840.
35. Matsushita, M., Tomizawa, K., Moriwaki, A., Li, S. T., Terada, H., and Matsui, H. (2001) A high-efficiency protein transduction system demonstrating the role of PKA in long-lasting long-term potentiation, *J. Neurosci. 21*, 6000−6007.
36. Richard, J. P., Melikov, K., Vives, E., Ramos, C., Verbeure, B., Gait, M. J., Chernomordik, L. V., and Lebleu, B. (2003) Cell-penetrating peptides. A reevaluation of the mechanism of cellular uptake, *J. Biol. Chem. 278*, 585−590.
37. Lundberg, M., Wikstrom, S., and Johansson, M. (2003) Cell surface adherence and endocytosis of protein transduction domains, *Mol. Ther. 8*, 143−150.
38. Wadia, J. S., Stan, R. V, and Dowdy, S. F. (2004) Transducible TAT-HA fusogenic peptide enhances escape of TAT-fusion proteins after lipid raft macropinocytosis, *Nat. Med. 10*, 310−315.
39. Zelphati, O., Wang, Y., Kitada, S., Reed, J. C., Felgner, P. L., and Corbeil, J. (2001) Intracellular delivery of proteins with a new lipid-mediated delivery system, *J. Biol. Chem. 276*, 35103−35110.
40. Yuki, S., Kondo, Y., Kato, F., Kato, M., and Matsuo, N. (2004) Noncytotoxic ribonuclease, RNase T1, induces tumor cell death via hemagglutinating virus of Japan envelope vector, *Eur. J. Biochem. 271*, 3567−3572.
41. Vogelstein, B., and Kinzler, K. W. (1992) p53 function and dysfunction, *Cell 70*, 523−526.
42. Verma, I. M., and Somia, N. (1997) Gene therapy—Promises, problems and prospects, *Nature 389*, 239−242.
43. Takenobu, T., Tomizawa, K., Matsushita, M., Li, S. T., Moriwaki, A., Lu, Y. F., and Matsui, H. (2002) Development of p53 protein transduction therapy using membrane-permeable peptides and the application to oral cancer cells, *Mol. Cancer Ther. 1*, 1043−1049.
44. Zender, L., Kuhnel, F., Kock, R., Manns, M., and Kubicka, S. (2002) VP22-mediated intercellular transport of p53 in hepatoma cells *in vitro* and *in vivo*, *Cancer Gene Ther. 9*, 489−496.
45. Michiue, H., Tomizawa, K., Wei, F. Y., Matsushita, M., Lu, Y. F., Ichikawa, T., Tamiya, T., Date, I., and Matsui, H. (2005) The NH_2 terminus of influenza virus hemagglutinin-2 subunit peptides enhances the antitumor potency of polyarginine-mediated p53 protein transduction, *J. Biol. Chem. 280*, 8285−8289.
46. Maeda, T., Mahara, K., Kitazoe, M., Futami, J., Takidani, A., Kosaka, M., Tada, H., Seno, M., and Yamada, H. (2002) RNase 3 (ECP) is an extraordinarily stable protein among human pancreatic-type RNases, *J. Biochem. 132*, 737−742.
47. Hartl, F. U., and Hayer-Hartl, M. (2002) Molecular chaperones in the cytosol: From nascent chain to folded protein, *Science 295*, 1852−1858.

BI052642A

Journal of Cellular Biochemistry 99:609–623 (2006)

Hydrogen Peroxide and Endothelin-1 are Novel Activators of Betacellulin Ectodomain Shedding

Michael P. Sanderson,[1,2]* Catherine A. Abbott,[1] Hiroko Tada,[3] Masaharu Seno,[3] Peter J. Dempsey,[4,5] and Andrew J. Dunbar[6]

[1]Cooperative Research Centre for Tissue Growth and Repair, School of Biological Sciences, Flinders University, Australia
[2]Tumor Immunology Programme, German Cancer Research Centre, Heidelberg, Germany
[3]Department of Bioscience and Biotechnology, Graduate School of Natural Science and Technology, Okayama University, Japan
[4]Pacific Northwest Research Institute, Seattle, Washington
[5]Department of Medicine, University of Washington, Seattle, Washington
[6]GroPep Limited, Adelaide, Australia

Abstract The betacellulin precursor (pro-BTC) is a novel substrate for ADAM10-mediated ectodomain shedding. In this report, we investigated the ability of novel physiologically relevant stimuli, including G-protein coupled receptor (GPCR) agonists and reactive oxygen species (ROS), to stimulate pro-BTC shedding. We found that in breast adenocarcinoma MCF7 cells overexpressing pro-BTC, hydrogen peroxide (H_2O_2) was a powerful stimulator of ectodomain shedding. The stimulation of pro-BTC shedding by H_2O_2 was blocked by the broad-spectrum metalloprotease inhibitor TAPI-0 but was still functional in ADAM17 (TACE)-deficient stomach epithelial cells indicating the involvement of a distinct metalloprotease. H_2O_2-induced pro-BTC shedding was blocked by co-culturing cells in the anti-oxidant N-acetyl-L-cysteine but was unaffected by culture in calcium-deficient media. By contrast, calcium ionophore, which is a previously characterized activator of pro-BTC shedding, was sensitive to calcium depletion but was unaffected by co-culture with the anti-oxidant, identifying a clear distinction between these stimuli. We found that in vascular smooth muscle cells overexpressing pro-BTC, the GPCR agonist endothelin-1 (ET-1) was a strong inducer of ectodomain shedding. This was blocked by a metalloprotease inhibitor and by overexpression of catalytically inactive E385A ADAM10. However, overexpression of wild-type ADAM10 or ADAM17 led to an increase in ET-1-induced pro-BTC shedding providing evidence for an involvement of both enzymes in this process. This study identifies ROS and ET-1 as two novel inducers of pro-BTC shedding and lends support to the notion of activated shedding occurring under the control of physiologically relevant stimuli. J. Cell. Biochem. 99: 609–623, 2006.

Key words: ADAM; betacellulin; ectodomain shedding; ErbB; endothelin; metalloprotease; reactive oxygen species

Abbreviations used: ADAM, a disintegrin and metalloprotease; APMA, *p*-aminophenylmercuric acetate; AR, amphiregulin; BTC, betacellulin; CM, conditioned media; DMEM, Dulbecco's modified Eagle's medium; DMSO, dimethyl sulfoxide; EGF, epidermal growth factor; EIA, enzyme-linked immunoassay; ER, epiregulin; ET-1, endothelin-1; FBS, fetal bovine serum; GPCR, G-protein coupled receptor; HB-EGF, heparin-binding EGF-like growth factor; HRP, horse radish peroxidase; MMP, matrix metalloprotease; NRG, neuregulin; PBS-T, phosphate buffered saline-tween; PSF, penicillin/streptomycin/fungizone; ROS, reactive oxygen species; SD, standard deviation; TACE, tumor necrosis factor-α-converting enzyme; TBS-T, Tris-buffered saline-tween; TGFα, transforming growth factor α; VSMC, vascular smooth muscle cell.

Grant sponsor: Australian Government Cooperative Research Centers Programme; Grant sponsor: National Institute of Health (NIH); Grant numbers: DK59778, DK63363; Grant sponsor: Crohn's and Colitis Foundation of America.

*Correspondence to: Michael P. Sanderson, Tumor Immunology Programme, D010, German Cancer Research Center, Im Neuenheimer Feld 280, D-69120 Heidelberg, Germany.
E-mail: m.sanderson@dkfz-heidelberg.de

Received 7 March 2006; Accepted 29 March 2006
DOI 10.1002/jcb.20968